HHS Public Access

Author manuscript

Immunity. Author manuscript; available in PMC 2024 December 12.

Published in final edited form as:

Immunity. 2023 December 12; 56(12): 2719–2735.e7. doi:10.1016/j.immuni.2023.11.003.

Intestinal microbiota-specific T_h17 cells possess regulatory properties and suppress effector T cells via c-MAF and IL-10

Leonie Brockmann[1], **Alexander Tran**[1], **Yiming Huang**[2,3], **Madeline Edwards**[1], **Carlotta Ronda**[3], **Harris H. Wang**[3,4], **Ivaylo I. Ivanov**[1,*]

[1]Department of Microbiology and Immunology, Vagelos College of Physicians and Surgeons, Columbia University, New York, NY 10032, USA

[2]Integrated Program in Cellular, Molecular, and Biomedical Studies, Columbia University, New York, NY 10032, USA

[3]Department of Systems Biology, Vagelos College of Physicians and Surgeons, Columbia University, New York, NY 10032, USA

[4]Department of Pathology and Cell Biology, Vagelos College of Physicians and Surgeons, Columbia University, New York, NY 10032, USA

Summary

Commensal microbes induce cytokine-producing effector tissue-resident CD4 T cells, but the function of these T cells in mucosal homeostasis is not well understood. Here we report that commensal-specific intestinal T_H17 cells possess an anti-inflammatory phenotype marked by expression of IL-10 and co-inhibitory receptors. The anti-inflammatory phenotype of gut-resident commensal-specific T_H17 cells was driven by the transcription factor c-MAF. IL-10-producing commensal-specific T_H17 cells were heterogeneous and derived from a $TCF1^+$ gut-resident progenitor T_H17 cell population. T_H17 cells acquired IL-10 expression and anti-inflammatory phenotype in the small intestinal lamina propria. IL-10-production by CD4 T cells and IL-10 signaling in intestinal macrophages drove IL-10 expression by commensal-specific T_H17 cells. Intestinal commensal-specific T_H17 cells possessed immunoregulatory functions and curbed effector T cell activity *in vitro* and *in vivo* in an IL-10-dependent and c-MAF-dependent manner. Our results suggest that tissue-resident commensal-specific T_H17 cells perform regulatory functions in mucosal homeostasis.

Introduction

Mucosal surfaces are colonized by a vast collection of resident microorganisms that shape tissue immune responses[1,2]. Intestinal tolerance towards commensals is promoted

*Corresponding author and Lead contact: Correspondence: Ivaylo I. Ivanov, ii2137@cumc.columbia.edu.

Author contributions

Conceptualization, L.B. and I.I.I.; methodology, L.B., A.T., Y.H., C.R., and I.I.I.; software, Y.H., A.T. and H.H.W.; formal analysis, L.B., A.T., Y.H., and I.I.I.; investigation, L.B., A.T., Y.H., M.E., and C.R.; resources, H.H.W. and I.I.I.; data curation, L.B., A.T., and Y.H.; writing – original draft, L.B. and I.I.I.; writing – review and editing, L.B. and I.I.I.; supervision, I.I.I.; funding acquisition, I.I.I.

Declaration of interests

H.H.W. is a scientific advisor of SNIPR Biome, Kingdom Supercultures and Fitbiomics, who were not involved in the study.

by induction of commensal-specific Foxp3$^+$ regulatory T cells[3–5]. However, commensals can also induce effector CD4 T cells, such as T_H17 cells[6–9]. The functions of commensal-specific T_H17 cells (hereafter referred to as commensal T_H17 cells) in mucosal immunity are incompletely understood. They can contribute to control of the inducing commensal[10], but whether they perform additional functions in mucosal homeostasis is unclear.

IL-17-producing CD4 T cells (T_H17 cells) are a functionally heterogeneous population and can acquire pathogenic and non-pathogenic phenotypes[11–15]. T_H17 cells are known drivers of inflammation, including intestinal inflammation, and can promote the pathology of inflammatory bowel diseases (IBD)[16,17]. However, not all T_H17 cells are inflammatory. For example, T_H17 cell-derived cytokines participate in strengthening the epithelial barrier and, therefore, in protection from inflammation[18–21]. T_H17 cells can also produce IL-10 and intestinal T_H17 cells can convert to a regulatory phenotype under inflammatory conditions[12,15,22]. Although inflammatory T_H17 cells have been well studied, the functions of non-pathogenic T_H17 cells are incompletely understood[23].

Gut-resident commensal T_H17 cells are metabolically distinct from inflammatory T_H17 cells[24] and are generally considered non-pathogenic. However, whether commensal T_H17 cells simply fail to participate in inflammatory responses or possess specific effector mechanisms to regulate inflammation that may direct additional functions in mucosal homeostasis is currently unknown.

Here, we examine in more detail the phenotype of various types of intestinal T_H17 cells, including commensal T_H17 cells induced by segmented filamentous bacteria (SFB). We find that SFB T_H17 cells possess a unique anti-inflammatory phenotype characterized by expression of the transcription factor c-MAF and the cytokine IL-10. Establishment of this program occurs in the terminal ileum and requires the coordinated action of intestinal CD4 T cells and intestinal macrophages. We also find that SFB T_H17 cells can curb effector T cell function both *in vitro* and *in vivo*. Our results describe anti-inflammatory functions of commensal T_H17 cells and suggest that these cells may have important roles in maintaining intestinal homeostasis.

Results

Small-intestinal commensal T_H17 cells have a regulatory transcriptional program

To identify unique features of commensal T_H17 cells, we profiled their transcriptome by RNA-sequencing and compared it to the transcriptome of alternatively generated intestinal T_H17 cells. *Il17a*^{GFP} reporter animals were colonized with SFB to induce commensal T_H17 cells (SFB T_H17 cells). Intestinal T_H17 cells were also induced by infecting *Il17a*^{GFP} animals with *Citrobacter rodentium* (*Crod*) or by transferring naïve CD45RB^{hi} CD4 T cells from *Il17a*^{GFP} animals to RAG1-deficient animals in a classical model of intestinal inflammation. Lamina propria (LP) T_H17 cells were isolated from small (SI) and large (LI) intestine at the peak of microbial colonization or colitis induction (Figure S1A–C). T_H17 cells comprised significant percentage of CD4 T cells in intestinal tissues (Figure 1A). However, T_H17 cell phenotype differed between the different conditions (Figure 1B). The transcriptional program of SFB-induced T_H17 cells was distinct from the transcriptional

programs of other intestinal T_H17 cells (Figure 1B). Expression of 500–1,100 genes differed significantly between SFB T_H17 cells and any other examined intestinal T_H17 cells (Figure S1D). In contrast, DEG numbers were lower in pairwise comparisons between non-SFB T_H17 cells (Figure S1E). We identified a core signature of 309 genes that differed significantly between SFB T_H17 cells and at least three of the other T_H17 cell datasets (Figure 1C and S1F). The core SFB T_H17 cell program contained genes involved in inhibitory/regulatory (e.g., *Ctla4, Lag3, Tigit*), anti-inflammatory (e.g., *Maf, Il10*) and tissue-protective (e.g., *Ahr, Areg*) functions (Figure 1D, E and S1G). At the same time genes enriched in inflammatory T_H17 cells were underrepresented in SFB T_H17 cells (Figure S1H). Overall, SFB T_H17 cells specifically expressed genes associated with decreased T cell responsiveness[25]. We, therefore, compared this program to the gene signatures of "non-responsive" T cells, such as exhausted and regulatory T cells. SFB T_H17 cells resembled exhausted CD4 T cells generated following chronic infection (Figure 1F)[26] and expressed classical markers of CD4 T cell exhaustion such as *Ikzf2* and *Tox*[27,28] (Figure 1E). At the same time, SFB T_H17 cells closely resembled mouse and human IL-10 expressing immunoregulatory T_H17 cells[12,29] (Figure 1G and S1I). Moreover, commensal-induced T_H17 cells were enriched in a subset of signature genes for IL-10^+Foxp3^{neg} T_R1 cells (Figure 1H). Comparison of core leading edge genes in SFB T_H17 cells to published mouse and human IL-10-expressing T_H17 cells and non-pathogenic T_H17 cells identified a set of 11 common genes, most notably genes encoding the prototypical anti-inflammatory cytokine IL-10, and the transcription factor c-MAF[30–32] (Figure 1I). Among intestinal T_H17 cells, expression of *Il10* transcripts was restricted to commensal T_H17 cells (Figure 1D and S1G) and *Maf* expression was significantly upregulated in SFB T_H17 cells (Figure 1E and S1G). In addition to *Maf*, several other transcription factors, including *Maf* co-factors, involved in regulation of *Il10* in CD4 T cells, such as *Ikzf3, Ahr* and *Nfil3*[33–35] were also expressed preferentially in commensal intestinal T_H17 cells (Figure 1E). Collectively, these results suggest that commensal intestinal T_H17 cells possess an anti-inflammatory transcriptional program that resembles that of IL-10-producing regulatory CD4 T cells.

Small-intestinal commensal T_H17 cells express IL-10 and co-inhibitory receptors

To confirm the RNA-Seq data we followed expression of IL-10 in commensal or non-commensal T_H17 cells using *Il10*^{GFP}/*Il17a*^{Katushka}/*Foxp3*^{mRFP} reporter mice. Non-commensal T_H17 cells lacked expression of IL-10 in SI and LI LP (Figure 2A, B and S2A). In contrast, ~40% of SFB-induced T_H17 cells in the small intestine co-expressed IL-17 and IL-10 (Figure 2A, B). *Citrobacter*-induced and colitogenic intestinal T_H17 cells produced IFN-γ and GM-CSF (Figure S2B, C). In contrast, commensal T_H17 cells lacked expression of these inflammatory cytokines (Figure S2B, C). We also examined expression of c-MAF in intestinal T_H17 cells by flow cytometry. SFB colonization induced significant increase in the proportion of T_H17 cells that co-expressed c-MAF and IL-17 (Figure 2C, D). On average, 50% of SI LP T_H17 cells in SFB-positive animals expressed c-MAF, which was similar to that of intestinal Foxp3^+ Tregs (Figure 2C, D). In contrast, other intestinal T_H17 cells demonstrated either no change or decrease in the proportion of c-MAF$^+$ cells (Figure 2C, D). The proportion of IL-10- and c-MAF-positive T_H17 cells was not specifically increased in LI LP of SFB-positive animals (Figure S2A, D). SFB colonization generally did not significantly increase the proportion of Foxp3^{neg}IL-17^{neg}IL-10^+ (T_R1) cells, although slight

increase was noted in the terminal ileum (Figure S2E). c-MAF induction in commensal T_H17 cells preceded IL-10 expression and c-MAF was already significantly upregulated in IL-10^{GFPneg} commensal T_H17 cells (Figure 2E). However, c-MAF expression further increased in IL-10^{GFP+} SFB-induced T_H17 cells (Figure 2F). Similarly to endogenous T_H17 cells, naïve SFB-specific 7B8 Tg CD4 T cells adoptively transferred into SFB-positive WT C57BL/6 mice, differentiated into IL-10- and c-MAF-expressing T_H17 cells (Figure 2G, H). c-MAF is a transcription factor known to promote IL-10 expression in T cells and non-pathogenic T_H17 cells[33,36]. In addition, c-MAF has been shown, in several other T cell subsets, to imbue anti-inflammatory functions, even beyond IL-10[25,36]. In particular, c-MAF controls an inhibitory gene module in CD4 and CD8 T cells that contains a number of co-inhibitory receptors, e.g. CTLA4, LAG3, TIM3, TIGIT[25]. In agreement with a crucial role for c-MAF, SFB T_H17 cells, but not other intestinal T_H17 cells, contained a population that co-expressed IL-10 and co-inhibitory receptors (Figure 2I, J). Analysis of c-MAF target genes[36] in our RNA-Seq datasets, showed that within the core SFB T_H17 cell signature, genes upregulated in SFB T_H17 cells were enriched in targets positively regulated by c-MAF and genes downregulated in SFB T_H17 cell were enriched in targets negatively regulated by c-MAF (Figure 1C). To investigate whether the induction of IL-10^+ T_H17 cells was restricted to SFB, we induced T_H17 cells in *Il10*^{GFP}/*Il17a*^{Katushka}/*Foxp3*^{mRFP} reporter mice by oral gavage of *Bifidobacterium adolescentis* (Figure S2F) [37]. *B. adolescentis* induced T_H17 cells in the SI LP, which similarly to SFB T_H17 cells, expressed IL-10 and c-MAF, as well as the co-inhibitory receptors CTLA-4 and LAG-3 (Figure 2K–M). Altogether our results suggest that c-MAF leads to expression of IL-10 and generally inhibitory T cell phenotype in commensal-specific SI LP T_H17 cells.

The anti-inflammatory phenotype of SFB T_H17 cells is driven by c-MAF

To directly assess the role of c-MAF in the acquisition of the T_H17 cell regulatory phenotype we conditionally deleted c-MAF in T_H17 cells by generating *Il10*^{GFP}/*Il17a*^{Katushka}/*Foxp3*^{mRFP}/*Il17a*^{Cre}/*Maf*$^{flox/flox}$/*R26*$^{STOP\text{-}YFP}$ mice (*Maf*$^{\Delta IL17}$). IL-17 expressing cells are also permanently labeled with YFP in these animals (Figure S3A). We confirmed T_H17 cell-specific deletion of c-MAF in SI LP T_H17 cells of *Maf*$^{\Delta IL17}$ mice (Figure 3A). SFB T_H17 cells were present in SI LP of *Maf*$^{\Delta IL17}$ mice, albeit at slightly decreased frequency compared to littermate controls (Figure 3B and S3B). Other T cell and IL-17-expressing subsets were unchanged with exception of a decrease in IL-17^+ γδ T cells (Figure S3C, D) as reported elsewhere [38]. c-Maf-deficiency in Foxp3^+ Tregs can also indirectly affect T_H17 cell function through loss of IL-10 expression on Tregs [39]. However, frequency and IL-10 production by Foxp3^+ Tregs were unaffected in *Maf*$^{\Delta IL17}$ mice (Figure 3C and S3C). In contrast, SFB T_H17 cells lacked IL-10 expression in *Maf*$^{\Delta IL17}$ mice compared to littermate controls (Figure 3C, D and S3C). Moreover, c-MAF-deficient SI LP T_H17 cells also lost, or downregulated, other signature genes of the SFB anti-inflammatory program (Figure 3D and S3E). Instead, SI LP SFB T_H17 cells from *Maf*$^{\Delta IL17}$ mice showed increased frequency of IFN-γ (Figure 3E) and up-regulated other genes associated with inflammatory T_H17 cells (Figure 3D and S3E)[40]. To examine changes in the overall transcriptional program, we performed single cell RNA-sequencing (scRNA-Seq) on purified YFP^+ T_H17 cells from SI LP of *Maf*$^{\Delta IL-17}$ mice and littermate controls following SFB colonization. c-MAF-deficient SFB T_H17 cells showed general loss of the SFB T_H17 signature anti-inflammatory program

(Figure 3F). In contrast to WT T_H17 cells, the transcriptional program of SFB T_H17 cells from *Maf*$^{\Delta IL17}$ mice resembled that of *Crod*-induced and colitogenic T_H17 cells in our bulk RNA-Seq datasets (Figure 3G), as well as that of published inflammatory EAE T_H17 cells (Figure S3F). These results suggest that acquisition of an anti-inflammatory phenotype by commensal T_H17 cells, including IL-10-expression, requires c-MAF.

Small-intestinal commensal T_H17 cells have immunoregulatory functions

The forgoing results demonstrate that SFB T_H17 cells express IL-10 and share transcriptional and phenotypic characteristics with IL-10-expressing immunoregulatory CD4 T cells, such as Foxp3^{neg} T_R1 cells. We, therefore, investigated whether commensal T_H17 cells can regulate the function of other CD4 T cells. To evaluate inhibitory effects on T cell proliferation, we compared the proliferation of responder CD4 T cells *in vitro* in the presence or absence of purified intestinal T_H17 cells. *Citrobacter*-induced T_H17 cells from small or large intestine did not significantly affect proliferation of responder T cells (Figure 4A). In contrast, co-culture with SFB-induced SI LP T_H17 cells led to significant inhibition of responder T cell proliferation (Figure 4A). Inhibition of proliferation did not correlate with preferential expansion of intestinal T_H17 cells in these assays, because despite showing higher inhibitory activity, SFB T_H17 cells demonstrated lower proliferative capacity than *Citrobacter* T_H17 cells (Figure 4B). Inhibition of proliferation by SFB T_H17 cells required IL-10 signaling, because it was virtually abrogated by addition of IL-10R-blocking antibody to the co-cultures (Figure 4C). Moreover, SFB T_H17 cells did not inhibit proliferation of responder CD4 T cells that lacked expression of IL-10R (Figure 4D). SFB T_H17 cells also express co-inhibitory receptors (Figure 2I, J). Blocking antibodies against CTLA-4, but not LAG-3, partially reduced the inhibitory ability of SI LP SFB T_H17 cells (Figure 4E, F). In addition, c-MAF-deficient SI LP SFB T_H17 cells lost the ability to suppress responder T cell proliferation (Figure 4G). These results suggest that intestinal commensal T_H17 cells can exert regulatory functions *in vitro* in an IL-10 and c-MAF-dependent manner.

To evaluate immunoregulatory functions of SFB T_H17 cells *in vivo* we considered their localization. SFB T_H17 cells are exclusively present in SI LP[6,41–43]. Compared to other T_H17 cells in our dataset, SFB T_H17 cells express a number of chemokine receptors, e.g. *Ccr9*, *Ccr5, Ccr1,* associated with tissue residency or homing to SI (Figure S3A)[44–46]. In addition, SFB T_H17 cells almost uniformly express the tissue retention factor CD69 (Figure S3B)[47]. Purified small-intestinal SFB T_H17 cells homed exclusively to the SI LP, but not to other tissues, including other intestinal tissues (Figure S3C). Thus, SFB T_H17 cells possess features of tissue-resident CD4 T cells. We, therefore, investigated whether SFB T_H17 cells exert immunoregulatory functions locally in the small intestine. Adoptive transfer of purified intestinal SFB T_H17 cells into RAG1-deficient animals (Figure 4H) significantly inhibited expansion (Figure 4I) and IL-17 production (Figure 4J, K) of co-transferred naïve 7B8 Tg CD4 T cells. The inhibition was similar to that exerted by SI LP Foxp3$^+$ Tregs (Figure 4I–K). Moreover, this inhibition occurred only in the SI LP and was not observed in mLN (Figure S3D). Neutralization of IL-10-signaling *in vivo*, significantly reduced commensal T_H17 cell-mediated inhibition of CD4 T cell expansion and cytokine production in SI LP (Figure 4I–K). The foregoing results suggest that commensal T_H17 cells can exert

immunoregulatory functions and curb effector T cell activity both *in vitro* and *in vivo* in an IL-10-dependent manner.

Commensal T_H17 cells are heterogeneous and contain a progenitor TCF1$^+$ subset

To further examine the heterogeneity of commensal T_H17 cells, we purified T_H17 cells from SI LP of SFB-colonized *Il17a*^{Katushka}/*Foxp3*^{mRFP} reporter mice and performed scRNA-Seq. Uniform Manifold Approximation and Projection for Dimensional Reduction (UMAP) analysis of 5721 recovered single SI LP T_H17 cells showed several transcriptionally distinct clusters (Figure 5A). We annotated these clusters into functional sets based on the genes that were differentially expressed relative to all other clusters (Figure 5B, C). Apart from two small clusters enriched in proliferation and interferon stimulated (ISG) genes respectively, the majority (97%) of intestinal T_H17 cells had terminally differentiated or progenitor/stem-like phenotypes (Figure 5B, C). Terminally differentiated T_H17 cells belonged to two distinct types with activated (C1, C3) and inhibitory (C2, C6) phenotypes respectively (Figure 5B, C). Activated T_H17 cells expressed genes associated with T cell activation and intestinal tissue residency, e.g. *Cd69, Cd28, Jun, Ccr9, Ccr2, Ccr5, Ccl20*. In contrast, T_H17 cells with inhibitory phenotype expressed inhibitory and tissue-repair genes, e.g. *Lag3, Tim3 (Havcr2), IL17f, Tgfb1, Areg* (Figure 5B). Cells in C1 and C6 contained higher expression of the corresponding effector programs (Figure 5B). Both types of terminally differentiated T_H17 cells contained cells expressing *Il10* (Figure 5D). Pathway analysis of differentially expressed genes demonstrated differences not only in activation, but also in their metabolic profile (Figure 5E). Metabolism is an established regulator of T cell functionality. We, therefore, applied the COMPASS algorithm[48] to compare metabolic states of the two most divergent IL-10-expressing clusters (C1 and C6). COMPASS predicted that cells in C1 had increased levels of glycolysis and those in C6 had increased fatty acid oxidation and amino acid metabolism (Figure 5F). These differences parallel those previously described between pathogenic T_H17 cells vs non-pathogenic T_H17 cells and Foxp3$^+$ Treg cells. c-MAF targets were specifically enriched in the two types of IL-10$^+$ T_H17 cells (Figure 5G). We next examined the role of c-MAF by purifying YFP$^+$ SI LP T_H17 cells from *Maf*$^{\Delta IL-17}$ mice and WT littermate controls and performing sc-RNA-Seq. Analysis of more than 10,000 SI LP T_H17 cells identified similar UMAP functional clustering (Figure S5A, B). Further analysis revealed that both types of IL-10$^+$ T_H17 cell subsets required c-MAF for IL-10 expression (Figure 5H). T_H17-specific deletion of c-MAF led to a decrease in the most differentiated IL-10$^+$ T_H17 cell clusters (Figure 5I, J). In addition, T_H17-specific deletion of c-MAF resulted in loss of the overall anti-inflammatory program of both activated and inhibitory effector IL-17$^+$ T_H17 cell subsets (Figure 5K and Figure S5C). In addition, conditional deletion of c-MAF resulted in a significant increase in the proportion of YFP$^+$IL-17^{neg} (ex-T_H17) cells with an inflammatory phenotype (Figure 5I–L and S5D). Thus, c-MAF not only drives the anti-inflammatory SFB T_H17 cell program, but also inhibits conversion into inflammatory ex-T_H17 cells.

Progenitor-like commensal T_H17 cells were defined by expression of stem-like features, e.g. *Tcf7, Il7r, and Slamf6*[49,50], with cluster C4 (Figure 5A) showing the highest combined expression of these genes (Figure 5A, 6A and S6A). We confirmed co-expression of TCF1 and IL-7R on a subset of commensal SI LP T_H17 cells by flow cytometry (Figure 6B).

In agreement with the scRNA-Seq data, TCF1 expression was downregulated in IL-10^{+} SFB T_H17 cells (Figure 6C). In contrast, a subset of TCF1^{+} SFB T_H17 cells expressed low levels of c-MAF (Figure 6D). Progenitor-like SI LP T_H17 cells had significantly decreased ability to suppress T cell proliferation *in vitro*, compared to TCF1^{neg} IL-10^{+} T_H17 cells (Figure 6E and S6B, C). Trajectory analysis of scRNA-Seq data from SI LP T_H17 cells revealed three distinct trajectories for progenitor-like TCF1^{+} T_H17 cells in cluster C4 leading respectively to the two effector IL-10^{+} populations, or back to the progenitor-like group (Figure 6F). This suggests that TCF1^{+} T_H17 cells have the potential to self-renew and are progenitors of TCF1^{neg}IL-10^{+} T_H17 cells. We also identified a similar TCF1^{+} T_H17 cell subset in the LI LP of animals infected with *Citrobacter rodentium* (Figure S6D, E). To confirm experimentally the progenitor nature of TCF1^{+} T_H17 cells, we generated *Tcf7*^{mCherry} reporter mice and crossed them to *Il17a*^{GFP} and *Il10*^{Venus} reporter animals (Figure S6F, G). Analysis of SI LP T_H17 cells confirmed that TCF1$^{mCherry+}$ T_H17 cells do not express IL-10 (Figure 6G, H). Next, we purified TCF1$^{mCherry+}$ T_H17 cells from SI LP of SFB-positive animals and adoptively transferred these cells into SFB-colonized wildtype mice. TCF1$^{mCherry+}$ T_H17 cells homed to SI LP immediately after transfer and gave rise to TCF1^{mCherryneg} T_H17 cells at later timepoints (Figure 6I). Purified SFB TCF1^{+} LP T_H17 cells also differentiated into TCF1^{neg}IL-10^{+} T_H17 cells upon TCR stimulation *in vitro*, in contrast to TCF1^{+} LP T_H17 cells from *Crod*-infected mice (Figure 6J). In these experiments, we could not recover TCF^{neg} T_H17 cells following adoptive transfer or *in vitro* culture, suggesting that they lose the ability to self-renew and to propagate an immune response (data not shown). Altogether the foregoing results suggest that IL-10^{+} commensal T_H17 cells in the SI LP are heterogeneous and differentiate from TCF1^{+} progenitor T_H17 cells that upregulate c-MAF and downregulate TCF1 expression.

To further examine the phenotype of TCF1^{+} progenitor T_H17 cells we performed bulk RNA-Seq analysis on purified TCF1^{+} and TCF1^{neg} SI LP T_H17 cells from SFB-colonized or *Crod*-infected *Tcf7*^{mCherry}/*Il17a*^{GFP} reporter mice. SFB TCF1^{+} T_H17 progenitors differed significantly from *Crod* T_H17 progenitors (Figure 6K, L). Gene set enrichment analysis showed that SFB TCF1^{+} progenitors were enriched in the core SFB anti-inflammatory signature compared to *Crod* TCF1^{+} progenitors, which resembled the general *Crod* T_H17 program (Figure 6M). For both types of microbes, the transcriptional program of progenitor T_H17 cells most closely resembled that of the corresponding TCF1^{neg} T_H17 cells (Figure 6K) with TCF1^{+} and TCF1^{neg} SFB T_H17 cells overlapping most closely and expressing the least number of differentially expressed genes (DEGs) (Figure 5K, L). SFB T_H17 cell signature anti-inflammatory genes were enriched in TCF1^{+} and TCF^{neg} T_H17 cells compared to *Crod* T_H17 cells and, vice versa, inflammatory markers were enriched in *Crod* TCF1^{+} T_H17 cells (Figure 6M, N and S6H). *Il10, Maf, Tox* and other genes associated with the SFB T_H17 program were already upregulated in TCF1^{+} SFB progenitors, and further increased in TCF^{neg} SFB effectors (Figure 6N, O and S6H, I). We next investigated whether inflammatory cytokines could affect the transcriptional program of commensal T_H17 progenitors. *In vitro* stimulation of purified SI LP TCF1^{+}IL-17^{+}IL-10^{neg} T_H17 cells in the presence of IL-1β and IL-23 resulted in significant decrease in their ability to differentiate into IL-10^{+} effector T_H17 cells (Figure 6P) and instead induced production of IFNγ (Figure 6Q). Combined our results suggest that LP TCF1^{+} progenitor commensal

T_H17 cells are transcriptionally poised to differentiate to anti-inflammatory effectors but retain the ability to respond to inflammatory queues from the environment.

IL-10 signaling and intestinal macrophages in terminal ileum instruct acquisition of T_H17 anti-inflammatory phenotype

We next investigated the signals and participating innate immune cells that facilitate the differentiation of $TCF1^+$ progenitors into IL-10-expressing anti-inflammatory T_H17 cells. $TCF1^+$ progenitor T_H17 cells were present exclusively in the SI LP and not in mLN, and adoptively transferred $TCF1^+$ progenitor T_H17 cells homed exclusively to the SI LP (Figure S7A). In addition, although $TCF1^+$ T_H17 cells were present in both duodenum and ileum, $TCF^{neg}IL\text{-}10^+$ T_H17 cells were specifically present in the terminal ileum (Figure 7A, B). Purified ileal $TCF1^+$ SFB T_H17 cells had a significantly increased capacity to generate $TCF1^{neg}$ $IL\text{-}10^+$ T_H17 cells *in vitro*, compared to $TCF1^+$ SFB T_H17 cells from duodenum or SI LP $TCF1^+$ T_H17 cells from *Citrobacter*-infected mice (Figure S7B). The foregoing results suggest that commensal precursor T_H17 cells acquire IL-10 expression locally in the terminal ileum under the guidance of signals from the gut microenvironment.

IL-10 induces T_R1 cell differentiation *in vitro*[51] and is required for the maintenance of IL-10 expression in T_R1 cells and $Foxp3^+$ Tregs[52,53]. We, therefore, investigated the role of IL-10 in generation of IL-10-producing SFB T_H17 cells. For this, we crossed $Il10^{GFP}/Il17a^{Katushka}/Foxp3^{mRFP}$ reporter mice to SFB-specific 7B8 TCR Tg mice on a Ly5.1 congenic background. We then adoptively transferred naïve 7B8.Ly5.1-triple reporter CD4 T cells into WT and IL-10-deficient animals and examined SFB-specific T_H17 cell induction, as well as the phenotype of the induced T_H17 cells (Figure 7C). 7B8 CD4 T cells differentiated into IL-10-expressing T_H17 cells in SI LP of WT control animals (Figure 7D). In contrast, although WT 7B8 CD4 T cells downregulated TCF1 and became T_H17 cells in $Il10^{-/-}$ mice, they had significantly decreased proportion of $IL\text{-}10^+$ T_H17 cells (Figure 7D and Figure S7C, D). Moreover, 7B8 CD4 T_H17 cells had decreased expression of c-MAF in the absence of environmental IL-10 (Figure 7E). Therefore, IL-10 is required for the induction of c-MAF and IL-10 in commensal T_H17 cells. To investigate the source of IL-10, we next transferred triple reporter 7B8 Tg CD4 T cells into recipients with conditional deletion of IL-10 in T cells ($Cd4^{Cre}/Il10^{flox/flox}$ or $Il10^{\Delta T}$ mice). Despite similar T_H17 cell differentiation, 7B8 T_H17 cells had decreased c-MAF and IL-10 expression in the absence of IL-10 production by T cells (Figure 7F, G and S7E). These results suggest that IL-10 production by CD4 T cells is required for induction of IL-10 expression by commensal T_H17 cells. To investigate whether IL-10 acts directly on the differentiating commensal T_H17 cells, we transferred control and $Il10rb^{-/-}$ triple reporter CD4 T cells into WT recipients (Figure 7H). IL-10Rβ-deficient CD4 T cells differentiated into T_H17 cells similarly to controls (Figure S7F) and contained similar proportion of $c\text{-}MAF^+$ and $IL\text{-}10^+$ T_H17 cells (Figure 7I and Figure S7G). In contrast, despite unimpeded T_H17 cell differentiation, WT SFB-specific CD4 T cells did not become $IL\text{-}10^+$ or $c\text{-}MAF^+$ T_H17 cells when transferred into IL-10Rβ-deficient recipients (Figure 7J, K and S7H). Combined, these results suggest that IL-10 does not directly act on differentiating commensal T_H17 cells. We previously reported that intestinal macrophages (iMf) participate in the induction of SFB-specific T_H17 cells[54]. Moreover, IL-10Rβ signaling in iMϕ is crucial for establishment

of intestinal homeostasis[55]. We, therefore, investigated whether IL-10Rβ signaling in iMϕ is required for induction of IL-10 expression by SFB T_H17 cells. To conditionally delete IL-10Rβ in iMϕ we generated mixed bone marrow (BM) chimeras in which lethally irradiated WT mice were reconstituted with a 1:1 BM mixture from CCR2-DTR and *Il10rb*$^{-/-}$ animals (Figure 7L). We previously showed that diphtheria toxin (DT) injection leads to specific loss of iMfϕ, but not intestinal dendritic cells (iDCs) in CCR2-DTR animals[54]. Administration of DT in the mixed chimeras leads to deletion of CCR2-DTR iMfϕ, but not *Il10rb*$^{-/-}$ iMfϕ, resulting in an iMfϕ population that specifically lacks IL-10Rb expression (Figure S7I). SFB-specific CD4 T cells differentiated into IL-10$^+$ T_H17 cells when transferred into DT-treated control CCR2-DTR:WT BM chimeras (Figure 7M). In contrast, although 7B8 CD4 T cells differentiated similarly to T_H17 cells in recipients with conditional deletion of IL-10Rβ in iMfϕ (Figure S7J), these T_H17 cells had significantly decreased IL-10 and c-MAF expression (Figure 7M, N). Altogether the foregoing results suggest that iMfϕ detect T cell-derived IL-10 to induce or maintain production of IL-10 by commensal T_H17 cells.

Discussion

T_H17 cells are defined by the expression of the signature cytokine IL-17A. Although T_H17 cells were originally described as pro-inflammatory, it is now appreciated that there is a considerable range in T_H17 cell functionality[12,13,15,22,48,49]. Homeostatic non-pathogenic T_H17 cells have been described, but their functions have not been defined. In the gut, the role of commensal-induced T_H17 cells is unclear. Although absence of SFB T_H17 cells leads to slight SFB increase in the gut lumen[10], control of SFB is mainly mediated by type 3 innate lymphoid cells[56]. SFB T_H17 cells were originally considered pro-inflammatory. However, it was later shown that SFB T_H17 cells possess a non-pathogenic transcriptional program[24]. Our results demonstrate that SFB T_H17 cells have a regulatory anti-inflammatory program and can produce IL-10. We further found that *Bifidobacterium adolescentis* induces T_H17 cells with a similar phenotype, which suggests that IL-10 production by T_H17 cells is characteristic of multiple commensal species. Thus, commensal T_H17 cells may also play role in maintaining mucosal homeostasis. Indeed, intestinal SFB T_H17 cells prevent metabolic disease in the context of diet-induced obesity[57]. In addition, herein we report that SFB T_H17 cells suppress intestinal effector T cell responses via IL-10.

Intestinal IL-10$^+$ T_H17 cells were previously reported in an experimental model of intestinal inflammation and shown to transdifferentiate to T_R1 cells[22]. SFB-induced IL-10$^+$ T_H17 cells in the current study also express T_R1-associated genes. However, using scRNA-Seq of YFP$^+$ CD4 T cells from *Il17a*^{Cre}/*R26*$^{STOP\text{-}YFP}$ mice we found few YFP$^+$ CD4 T cells without IL-17 transcripts (ex-T_H17 cells) in WT animals, and therefore little evidence for trans-differentiation of SFB T_H17 cells at steady state. This is also in agreement with a prior study that concluded that SI LP SFB T_H17 cells possess little plasticity[24]. In contrast, after T_H17-specific ablation of c-MAF we found a considerable population of ex-T_H17 cells, which expressed pro-inflammatory genes. Therefore, c-MAF not only maintains IL-10 expression in commensal T_H17 cells, but also prevents trans-differentiation into pro-inflammatory CD4 T cells. Whether commensal T_H17 cells can become fully functional T_R1 cells remains to be investigated.

In our study, SFB T_H17 cells inhibited expansion and cytokine production of effector CD4 T cells in an IL-10 and c-MAF-dependent manner. However, they expressed several inhibitory receptors. Indeed, in our hands, blockade of CTLA-4, but not LAG-3, also partially inhibited suppression in the *in vitro* assay. Therefore, commensal T_H17 cells may possess additional mechanisms for maintaining T cell homeostasis, besides IL-10. In addition, in our *in vivo* experiments SFB T_H17 cells suppressed SFB-specific CD4 T cells. Therefore, whether commensal T_H17 cells can regulate non-cognate CD4 T cells remains to be investigated.

c-MAF plays divergent roles in the specialization of IL-17 producing T cells. c-MAF is not essential for RORγ expression in T_H17 cells and T_H17 cell differentiation[38]. However, c-MAF is activated early during T_H17 cell polarization together with T_H17-defining transcription factors and can act as a negative regulator[36]. In contrast, c-MAF is required for the development of RORγt$^+$ regulatory T cells and for the specialization of IL-17$^+$ γδ T cells, where it acts as an activator[38,58,59]. Regardless of its overall role, c-MAF is universally linked to positive regulation of IL-10 expression in T cells, including T_H17 cells[36,58]. Here, we find that c-MAF is required for the production of IL-10 by commensal T_H17 cells. Moreover, c-MAF was required not only for IL-10 production, but in general for the maintenance of the anti-inflammatory program of commensal T_H17 cells. This included the expression of tissue repair factors and co-inhibitory receptors. T_H17 cell-specific ablation of c-MAF led to expansion of IFNγ$^+$ T_H17 cells and IL-17^{neg} ex-T_H17 cells with a pro-inflammatory T_H1 phenotype. Thus c-MAF may also maintain the anti-inflammatory phenotype of commensal T_H17 cells by restricting inflammatory cytokines and T_H17 cell plasticity.

We find that IL-10$^+$ T_H17 cells were only present in the terminal ileum. Therefore, signals in this location likely mediate the induction or maintenance of their anti-inflammatory program. We previously showed that intestinal epithelial cells and intestinal macrophages play crucial roles in SFB T_H17 cell induction[54,60]. Here, we find that ablation of IL-10Rβ in macrophages perturbs induction of anti-inflammatory T_H17 cells but does not affect overall T_H17 cell differentiation. Therefore, intestinal macrophages are required for the induction or maintenance of anti-inflammatory T_H17 cells. IL-10Rβ signaling in macrophages is required for maintenance of intestinal homeostasis[55]. Our data suggest that maintenance of anti-inflammatory commensal T_H17 cells may contribute to the mechanisms by which resident macrophages suppress gut inflammation. Although the exact source of IL-10 required for iMϕ activation remains to be ascertained, we find that IL-10 from CD4 T cells is required for the presence of IL-10$^+$ T_H17 cells. Both Foxp3$^+$ Tregs and Foxp3^{neg} T_R1 cells can produce IL-10 thus establishing an interdependent network of IL-10 producing CD4 T cells in mucosal homeostasis.

Pathogens induce quantitatively different T cell responses in the context of acute versus chronic infection. Whether commensals engage adaptive immunity in an acute or chronic manner is not known. In agreement with the expression of IL-10 and generally inhibitory or non-responsive program, commensal T_H17 cells closely resembled exhausted T cells induced during chronic infection. Therefore, in terms of T cell responses, presence of commensals resembles chronic infection. We also found significant heterogeneity of commensal T_H17 cells and the existence of a precursor TCF1$^+$ T_H17 cell population in the

SI LP that generates TCF1^{neg} IL-10^{+} T_H17 cells. Similar TCF1^{+} progenitor CD4 and CD8 T cells maintain TCF^{neg} effector responses in the context of chronic viral infections[61,62], further underscoring the similarities between homeostatic commensal and chronic infection T cell responses. SFB TCF1^{+} progenitor T_H17 cells were transcriptionally distinct from TCF1^{+} T_H17 cells during *Citrobacter rodentium* infection. Even though they retained the potential to generate inflammatory T_H17 cells, intestinal TCF1^{+} T_H17 cells closely resembled their TCF1^{neg} counterparts. Therefore, they were already poised towards an anti-inflammatory program. Our results suggest that this happens in the SI LP under the control of the local microenvironment. The specific signals controlling this transition, as well as the earliest events leading to the establishment of the SFB T_H17 cell differentiation program will be important to elucidate in future studies.

TCF^{neg} commensal T_H17 cells possessed inhibitory or activated phenotype and contained both IL-10^{+} and IL-10^{neg} T_H17 cells. Therefore, individual commensals generate heterogeneous T cell responses. We identified two unique subsets of IL-10^{+} T_H17 cells, both of which required c-MAF for IL-10 production. Whether these two subsets perform different functions or whether commensal T_H17 subsets with distinct functions co-exist, will be important to elucidate in future studies.

Our results describe an inherent heterogeneity of the T_H17 cell response to commensal microbes and show that such response may function not only in antigen-specific control of the inducing commensal, but also in general regulation of intestinal T cells in maintaining anti-inflammatory tone of the intestinal mucosa.

STAR Methods text

Lead contact

Further information and requests for resources and reagents should be directed to and will be fulfilled by the lead contact, Ivaylo Ivanov (ii2137@cumc.columbia.edu).

EXPERIMENTAL MODEL AND SUBJECT DETAILS

Animals

C57BL/6J, Ly5.1 (CD45.1), RAG1-deficient, *Il17a*^{GFP}, *Il17a*^{Cre}, *Il10*^{GFP}, *Foxp3*^{mRFP}, *Il10*$^{-/-}$, *Il10rb*$^{-/-}$ and 7B8 transgenic mice were purchased from the Jackson Laboratory. Animals were purchased only from SFB-negative maximum barrier rooms at Jackson. All animals were tested for SFB upon arrival and maintained in an SFB-negative high barrier room at Columbia University. 7B8 mice were bred to Ly5.1 and *Il17a*^{GFP} mice at Columbia University. *Il17a*^{Katushka} mice[63,64] were provided by Dr. Samuel Huber, Medical Center Hamburg-Eppendorf (UKE) with permission from Dr. Richard Flavell, Yale and bred at Columbia University. 7B8 mice were bred to Ly5.1 and to *Il10*^{GFP}/*Il17a*^{Katushka}/*Foxp3*^{mRFP} mice at Columbia University. *Maf*$^{fl/fl}$ on C57BL/6 background were obtained from Dr. Nicola Gagliani, University Medical Center Hamburg-Eppendorf and Dr. Arnold Han, Columbia University with permission from Dr. Carmen Birchmeier and bred at Columbia University. *Ccr2*^{DTR} mice[65] were gifted by Dr. Eric Parmer, Memorial Sloan-Kettering Cancer Center. *Il10*^{flox} mice[66] were obtained from Dr. A. Roers, Technische Universitat

Dresden and bred to *Cd4*^{Cre} mice at Columbia University. *Il10*^{Venus} mice[4] were gifted by Dr. Kenya Honda, Keio University with permission from Dr. Kiyoshi Takeda, Osaka Unviersity and bred to *Tcf7*^{mCherry} mice at Columbia University. *Tcf7*^{mCherry} mice were generated using CRISPR/Cas9 based gene editing in C57BL/6J mice. The targeted vector contains an mCherry reporter sequence preceded by a splice acceptor site and a P2A self-cleaving sequence placed in intron 2 and surrounded by a pair of non-complementary *LoxP* sites (Figure S5). The targeting construct also contained an inversion of the *Tcf7* genomic sequence containing Exons 3–4 surrounded by two pairs of *LoxP* and *LoxP2272* sequences in opposite orientation in intron 2 and intron 5. The targeted reporter allele therefore expresses mCherry and is a functional knock-out for TCF1 that can be conditionally activated upon expression of Cre-recombinase (Figure S5). Cre-recombinase was not used in this study and all animals used were heterozygous or *Tcf7*$^{mCherry/+}$. All mouse strains were bred and housed under specific pathogen-free conditions at Columbia University Medical Center under IACUC approved guidelines. To control for microbiota and cage effects, experiments were performed with gender matched littermate control animals that were housed in the same cage.

METHOD DETAILS

SFB colonization and quantification

SFB colonization was performed by single oral gavage of fecal suspension from SFB-enriched mice as previously described[42]. To control for variability in SFB levels in feces used for gavage, all gavages were performed with frozen stocks from a single batch of SFB-enriched feces. Fecal samples were tested for SFB by quantitative RT-PCR and frozen as batch aliquots at −80C. Control SFB-negative feces were collected in a similar manner. SFB colonization levels were confirmed by qPCR and normalized to levels of total bacteria (UNI) as previously described[42].

***Citrobacter rodentium* infection—**Mice where infected with 1×10^9 CFU of *Citrobacter rodentium* by oral gavage. Infection was confirmed by measuring CFU in fecal samples throughout the course of infection.

***Bifidobacterium adolescentis* and *Escherichia coli* gavage—**Mice were gavaged with *Bifidobacterium adolescentis* (*Ba*) or Escherichia coli (*Ec*) every other day for 14 days. *Ba* was grown in Reinforced Clostridial Medium in an anaerobic chamber (5% H_2, 10% CO_2, 85% N_2) at 37C for 48 hours. *Ec* was grown overnight in Luria-Bertani (LB) broth at 37C. *Ba* and *Ec* were gavaged in 200 µl PBS/mouse. Mice received 1×10^8 CFU/ml per gavage of either *Ba* or *Ec*.

Transfer colitis

FACS-sorted CD45RB^{high} CD4 T cells from spleen and lymph nodes were injected i.v. (5×10^5 cells/mouse) into RAG1-deficient mice. Lipocalin-2 in fecal samples was measured by ELISA.

***In vitro* suppression assay—**Responder naïve CD4 T cells (WT or *Il10rb*$^{-/-}$) isolated from spleen were purified via FACS (CD4^{+}TCRβ^{+}CD62^{+}CD44^{neg}CD25^{neg}). Responder CD4 T cells were labeled with 5 μM CellTrace violet dye (proliferation dye, Invitrogen) and stimulated in the presence of irradiated splenic APCs (25 Grey) and 1 μg/ml soluble anti-CD3 (clone 2C11). Responder CD4 T cells were cultured in the absence or presence of indicated SI LP CD4 T cells in a 2:1 ratio for 4 days. SFB and *Crod* T_H17 cells (CD4^{+}TCRβ^{+}IL-17^{GFP+}) were isolated from SI LP or LI LP of *Il17a*^{GFP} reporter mice two weeks after SFB gavage or *Crod* infection respectively. Foxp3^{+} Treg cells were isolated from SI LP of *Foxp3*^{mRFP} reporter mice. To assess the role of IL-10 signaling and co-inhibitory receptors, blocking antibodies against IL-10R, CTLA-4 or LAG-3 were added to some of the cell culture (anti-mouse IL-10R (1B1.3A), 10 μg/ml, Bio X Cell; anti-mouse CTLA-4 (63828), 10 μg/ml, R&D Systems; anti-mouse LAG-3 (C9B7W), 10 μg/ml, Bio X Cell). Division Index (DI) was calculated with FlowJo based on the divisions of responder T cells. Percent suppression was calculated using the following formula:

$$\% \text{ suppression} = 100 - 100\text{x (DI (responder+suppressor)/DI (responder alone))}$$

***In vivo* suppression assay—**Naïve 7B8 CD4 T cells were isolated from spleen of 7B8.Ly5.1 *Il17a*^{GFP} transgenic mice (Ly5.1) by FACS (Ly5.1^{+}Vβ14^{+}CD4^{+}TCRβ^{+}CD62L^{+}CD44^{neg}CD25^{neg}). Intestinal SFB T_H17 cells (CD4^{+}TCRβ^{+}IL-17^{GFP+}) and Foxp3^{+} Treg (CD4^{+}TCRβ^{+}Foxp3^{mRFP+}IL-17^{Katushkaneg}) cells were isolated from SI LP of *Il17a*^{GFP} or *Foxp3*^{mRFP} Ly5.2 mice respectively by FACS two weeks after SFB colonization. 30,000 naïve 7B8 CD4 T cells and 30,000 SI LP cells were injected intravenously in a 1:1 ratio into SFB-colonized *Rag1*$^{-/-}$ mice. Expansion and T_H17 cell differentiation of Ly5.1^{+} 7B8 CD4 T cells was analyzed in SI LP and mLN on day 8 post transfer. To assess the role of IL-10 signaling, anti-IL-10R antibody (200 μg/mouse clone 1B13A, Bio X Cell) or an isotype control antibody were injected on day 2, 4 and 6 post transfer.

Adoptive transfers

SFB-negative WT, *Il10*$^{-/-}$, *Il10rb*$^{-/-}$, or *Il10*$^{\Delta T}$ mice were gavaged with SFB-containing fecal pellets as described above. Five days after gavage, MACS-purified (CD4 beads, Miltenyi) 7B8 or total CD4 T cells from spleen and LN of SFB-negative (naïve) 7B8.Ly5.1 *Il10*^{eGFP}/*Il17a*^{Katushka}/*Foxp3*^{mRFP} or Ly5.1 *Il10*^{eGFP}/*Il17a*^{Katushka}/*Foxp3*^{mRFP} mice were transferred intravenously (5×10^5 7B8 cells/recipient or 2×10^6 total CD4 T cells/recipient).

Migration assays

Il17a^{GFP} reporter mice or *Tcf7*^{mCherry}/*Il17a*^{GFP} double reporter mice were gavaged with SFB-containing feces as described above. Two weeks after gavage, SI LP lymphocytes were isolated and SFB T_H17 cells (Ly5.1^{+}CD4^{+}TCRβ^{+}IL-17^{GFP+}) or TCF1^{+} SFB T_H17 cells (Ly5.1^{+}CD4^{+}TCRβ^{+}IL-17^{GFP+}TCF1$^{mCherry+}$) were FACS-purified. 50,000 SI LP T_H17 cells (combined from multiple mice) were injected intravenously into SFB-colonized WT mice (Ly5.2). Cells were isolated from mLN, LI LP, SI LP and liver at indicated timepoints to examine transferred Ly5.1^{+} CD4 T cell.

Mixed bone marrow chimeras

Total bone marrow cells were isolated from *Ccr2*^{DTR} mice, *Il10rb*$^{-/-}$ and WT C57BL/6 mice (all Ly5.2). After removal of red blood cells, *Ccr2*^{DTR} bone marrow cells were mixed in a 1:1 ratio with *Il10rb*$^{-/-}$ or WT bone marrow cells and five million total cells were transferred into lethally irradiated (11 Grey) recipient WT Ly5.1 mice. 12 weeks later, mice were colonized with SFB as described above. The mice were treated with 20 ng/g diphtheria toxin (DT) every other day starting on Day −1. Ly5.1/Ly5.2 7B8 triple reporter CD4 T cells were transferred on Day 0 as described earlier. T_H17 cell differentiation in SI LP was analyzed on Day 7. For Q-PCR analysis, intestinal cells were FACS-purified and sorted into TRIZOL reagent (Life technology).

Lymphocyte isolation from intestine

Lamina propria lymphocytes isolation from intestine was performed as previously described[42]. In brief, Peyer's patched (SI) were removed and intestines were opened longitudinally. After washing, the intestines were cut into 1 cm long pieces and incubated in 5 mM EDTA solution twice for 20 min at 37°C. Lamina propria lymphocytes were isolated by digesting the tissue with Collagenase D, DNAse and Dispase three times for 20 min at 37°C. Lymphocytes were further purified using 80:40 Percoll gradient.

In vitro* culture—Tcf7*^{mCherry}/*Il17a*^{GFP}/*Il10*^{Venus} triple reporter mice were gavaged with SFB-containing feces or infected with *Citrobacter rodentium* as described above. Lymphocytes were isolated two weeks later from terminal ileum (distal quarter of SI) or duodenum (proximal quarter of SI) (SFB-gavaged) or LI LP (*Crod*-infected). TCF1$^+$ T_H17 cells (CD4$^+$TCRβ$^+$IL-17^{GFP+}TCF1$^{mCherry+}$IL-10^{Venusneg}) were FACS-purified from individual mice and plated in 96-well plates coated with 5 μg/ml aCD3 antibody (clone 2C11) in the presence of 5 μg/ml soluble aCD28 antibody (clone 37.51) for four days. Additionally, FACS-sorted SFB TCF1$^+$ T_H17 cells (CD4$^+$TCRβ$^+$IL-17^{GFP+}TCF1$^{mCherry+}$IL-10^{Venusneg}) were plated in 96-well plates coated with 5 μg/ml aCD3 antibody (clone 2C11) in the presence of 5 μg/ml soluble aCD28 antibody (clone 37.51), 10 ng/ml IL-23 and 10 ng/ml IL-1β for four days.

Lipocalin-2 ELISA

Lipocalin-2 was measured in fecal pellets from colitogenic mice. Fecal pellets were weight and disrupted in PBS containing cOmplete protease inhibitor (Roche). After centrifugation, supernatant was collected and stored in −80C until Lipocalin-2 ELISA was performed. ELISA was performed according to manufacturer protocol.

IFN-γ ELISA

Cell culture supernatants were collected from *in vitro* cultures of SFB TCF1$^+$ T_H17 cells after four days in the presence or absence of IL-23 and IL-1β. IFN-γ ELISA was performed according to the manufacturer protocol.

Flow Cytometry

After isolation cells were analyzed immediately by flow cytometry. For intracellular cytokine and transcription factor staining, the cells were re-stimulated with PMA/Ionomycin for 3 hours in the presence of Brefeldin A, followed by fixation and permeabilization using Foxp3/transcription factor staining buffer kit (Tonbo) according to manufacturer protocol. Dead cells were excluded with fixable viability dye (eFluor506, Invitrogen).

Quantitative PCR

mRNA from FACS-sorted cells was isolated using TRIZOL reagent (Life technology) according to the manufacturer protocol. Reverse transcription was performed with QScript cDNA SuperMix (QuantaBio). Q-PCR was performed using SYBR Green on LightCycler 480 (Roche). Samples were analyzed using the ΔΔCt method and normalization to *Gapdh*.

Bulk RNA-sequencing and analysis

LP TCRβ^{+}CD4^{+}IL-17^{GFP} T_H17 cells were purified via FACS from small or large intestine two weeks after gavage with SFB or infection with *Citrobacter rodentium*, or 10 weeks after colitis induction (CD45RB^{hi} colitis). Total mRNA was isolated using TRIZOL (Life technology) as per the manufacturer protocol. RNA-sequencing (RNA-Seq) was performed at the JP Sulzberger Columbia Genome Center. RNA amplification and library preparation was performed using the CLONTECH kit by Takara Bio. Libraries were then sequenced using Illumina NovaSeq 6000 (~40M reads). RTA (Illumina) was used for base calling and bcl2fastq2 (version 2.20) for converting BCL to FASTQ format. Raw reads were then processed by Cutadapt v2.1 with the following parameters: '--minimum-length 30:30 -u 15 -u −5 -U 15 -U −5 -q 20 --max-n 0 --pair-filter=any' to remove low-quality bases and Illumina adapters. Next, pseudoalignment was performed against the index created from mouse transcriptomes (GRCm38) using Kallisto (0.44.0). Differential gene expression analysis was performed by DESeq2 using reads count estimated by pseudoalignment, and the sets of significantly differentially expressed genes were identified using the following steps: First, genes that were not significantly changed were excluded (padj < 0.05). Next, genes with very low expression level (transcripts per million, TPM < 5 in at least 9 out of the 10 samples) were also excluded. Finally, an unusually high level of Ig gene transcripts was observed in a few samples and, therefore, Ig genes were excluded from the analysis.

Gene set enrichment analysis (GSEA)

To identified if curated signature gene sets or other specific gene sets are significantly up-regulated or down-regulated compared to published datasets, we performed gene set enrichment analysis. Briefly, normalized gene expression levels by microarray or RNA-seq were obtained from NCBI Gene Expression Omnibus or the original publication. Next, fold-changes of gene expression between comparisons were calculated in R v.4.1.0, and normalized enrichment scores as well as p-values of given gene sets were then estimated using the fgsea R package v.1.24.0 with the setting "nperm=1000".

Identification of c-MAF target genes

To identify potential c-MAF target genes, we extracted results from a regulatory network analysis for T_H17 cell[36] that integrated ChIP-seq data and RNA-seq data. Briefly, the summed scores for KC network of c-MAF were extracted from the original publication and genes with a score greater than 2 were defined as c-MAF target genes.

Single cell RNA-sequencing and analysis

SI LP SFB T_H17 cells ($TCR\beta^+CD4^+Foxp3^{mRFPneg}IL\text{-}17^{Katushka+}$) were FACS-sorted from SFB-colonized *Il10*^{eGFP}/*Il17a*^{Katushka}/*Foxp3*^{mRFP} mice. In a second set of experiments, T_H17 cells ($TCR\beta^+CD4^+IL\text{-}17^{YFP+}$) were FACS-sorted from SI LP of *Foxp3*^{mRFP}/*Il17a*^{Cre}/*Maf*$^{flox/flox}$/*R26*$^{STOP\text{-}YFP}$ mice (*Maf*$^{\Delta IL17}$) (n=2) and *Foxp3*^{mRFP}/*Il17a*^{Cre}/*Maf*$^{flox/+}$/*R26*$^{STOP\text{-}YFP}$ (WT) mice (n=3) two weeks after SFB gavage. Prior to sorting, cells from individual animals were labelled using hashtag antibodies conjugated to nucleotide barcodes (BioLegend, #155831, #155833, #155835). scRNA-seq was performed at the JP Sulzberger Columbia Genome Center using the 10X Genomics platform with a target of 5,000 nuclei per sample and 130M reads. Next, reads alignment, filtering, and barcode counting were performed using Cell Ranger v.3.0.2. All single-cell analyses were performed using R v.4.1.0 and Python v.3.6. Briefly, Seurat v.4.0.5 was utilized for preprocessing, normalization, and clustering. Ggplots2 v.3.3.5 was used to generate UMAP and dot plots. Low quality cell profiles were excluded if they met one of the following criteria: (i) number of genes expressed 200 or 2500 or (ii) 5% of the total unique molecular identifiers (UMIs) were mitochondrial RNA. The data was then normalized using the NormalizeData function. Wild type and *Maf*$^{\Delta IL17}$ T_H17 cells were integrated using the SCTransform and FindIntegrationMarkers. Next, the RunPCA function was applied followed by FindNeighbors and FindClusters functions on the number of PCs selected using the ElbowPlot function. Marker genes that were differentially expressed within each cluster were identified by the FindAllMarkers function with average log-transformed fold change cutoffs of 0.25 and pct cutoffs of 0.25. Gene set scoring was performed using the VISION R package v.3.0.0[67]. Gene set enrichment scores and p-values were computed using the fgsea R package v.1.24.0, a fast algorithm for Gene Set Enrichment Analysis (GSEA). Genes were ranked utilizing the wilcoxauc function from the presto R package, which performs a Wilcoxon rank sum test. COMET Python package[68] was applied to predict cell surface markers for clusters of interest. COMPASS Python package[48] was applied to characterize cellular metabolic states for clusters of interest. Slingshot v.2.2.0[69] was used for trajectory analysis starting at the progenitor-like population (C4).

QUANTIFICATION AND STATISTICAL ANALYSIS

Statistical significance was determined by unpaired t test with Welch's correction or other methods as noted on figure legends. P values are represented on figures as follows: ns, not significant, * $p < 0.05$, ** $p < 0.01$, *** $p < 0.005$, **** $p < 0.001$, ***** $p < 0.0005$. Error bars on all figures represent standard error of the mean. Statistical analysis was performed using GraphPad Prism version 9.1 for Windows (GraphPad Software).

Supplementary Material

Refer to Web version on PubMed Central for supplementary material.

Acknowledgements

We thank Samuel Huber and Nicola Gagliani (UKE) for providing key mouse lines. We thank members of the Ivanov lab for technical help. This work was supported by funding from NIH (DK098378, AI144808, AI163069, AI146817) and Burroughs Wellcome Fund (PATH1019125) to I.I.I.. L.B. was partially supported by a fellowship from the German Research Foundation (DFG) (BR 6094/1–1). H.H.W. acknowledges funding from NSF (MCB-2025515), NIH (R01AI132403, R01DK118044, R01EB031935), Burroughs Wellcome Fund (PATH1016691), and the Irma T. Hirschl Trust.

References

1. Ivanov II, Tuganbaev T, Skelly AN, and Honda K (2022). T Cell Responses to the Microbiota. Annual review of immunology 40, 559–587. 10.1146/annurev-immunol-101320-011829.
2. Hooper LV, Littman DR, and Macpherson AJ (2012). Interactions between the microbiota and the immune system. Science 336, 1268–1273. 10.1126/science.1223490. [PubMed: 22674334]
3. Lathrop SK, Bloom SM, Rao SM, Nutsch K, Lio CW, Santacruz N, Peterson DA, Stappenbeck TS, and Hsieh CS (2011). Peripheral education of the immune system by colonic commensal microbiota. Nature 478, 250–254. 10.1038/nature10434. [PubMed: 21937990]
4. Atarashi K, Tanoue T, Oshima K, Suda W, Nagano Y, Nishikawa H, Fukuda S, Saito T, Narushima S, Hase K, et al. (2013). Treg induction by a rationally selected mixture of Clostridia strains from the human microbiota. Nature 500, 232–236. 10.1038/nature12331. [PubMed: 23842501]
5. Nutsch KM, and Hsieh CS (2012). T cell tolerance and immunity to commensal bacteria. Current opinion in immunology 24, 385–391. 10.1016/j.coi.2012.04.009. [PubMed: 22613090]
6. Ivanov II, Atarashi K, Manel N, Brodie EL, Shima T, Karaoz U, Wei D, Goldfarb KC, Santee CA, Lynch SV, et al. (2009). Induction of intestinal Th17 cells by segmented filamentous bacteria. Cell 139, 485–498. 10.1016/j.cell.2009.09.033. [PubMed: 19836068]
7. Ivanov II, Frutos Rde L, Manel N, Yoshinaga K, Rifkin DB, Sartor RB, Finlay BB, and Littman DR (2008). Specific microbiota direct the differentiation of IL-17-producing T-helper cells in the mucosa of the small intestine. Cell Host Microbe 4, 337–349. [PubMed: 18854238]
8. Atarashi K, Tanoue T, Ando M, Kamada N, Nagano Y, Narushima S, Suda W, Imaoka A, Setoyama H, Nagamori T, et al. (2015). Th17 Cell Induction by Adhesion of Microbes to Intestinal Epithelial Cells. Cell 163, 367–380. 10.1016/j.cell.2015.08.058. [PubMed: 26411289]
9. Gaboriau-Routhiau V, Rakotobe S, Lecuyer E, Mulder I, Lan A, Bridonneau C, Rochet V, Pisi A, De Paepe M, Brandi G, et al. (2009). The key role of segmented filamentous bacteria in the coordinated maturation of gut helper T cell responses. Immunity 31, 677–689. [PubMed: 19833089]
10. Kumar P, Monin L, Castillo P, Elsegeiny W, Horne W, Eddens T, Vikram A, Good M, Schoenborn AA, Bibby K, et al. (2016). Intestinal Interleukin-17 Receptor Signaling Mediates Reciprocal Control of the Gut Microbiota and Autoimmune Inflammation. Immunity 44, 659–671. 10.1016/j.immuni.2016.02.007. [PubMed: 26982366]
11. Ghoreschi K, Laurence A, Yang XP, Tato CM, McGeachy MJ, Konkel JE, Ramos HL, Wei L, Davidson TS, Bouladoux N, et al. (2010). Generation of pathogenic T(H)17 cells in the absence of TGF-beta signalling. Nature 467, 967–971. 10.1038/nature09447. [PubMed: 20962846]
12. Esplugues E, Huber S, Gagliani N, Hauser AE, Town T, Wan YY, O'Connor W Jr., Rongvaux A, Van Rooijen N, Haberman AM, et al. (2011). Control of TH17 cells occurs in the small intestine. Nature 475, 514–518. 10.1038/nature10228. [PubMed: 21765430]
13. Gaublomme JT, Yosef N, Lee Y, Gertner RS, Yang LV, Wu C, Pandolfi PP, Mak T, Satija R, Shalek AK, et al. (2015). Single-Cell Genomics Unveils Critical Regulators of Th17 Cell Pathogenicity. Cell 163, 1400–1412. 10.1016/j.cell.2015.11.009. [PubMed: 26607794]
14. El-Behi M, Ciric B, Dai H, Yan Y, Cullimore M, Safavi F, Zhang GX, Dittel BN, and Rostami A (2011). The encephalitogenicity of T(H)17 cells is dependent on IL-1- and IL-23-

induced production of the cytokine GM-CSF. Nature immunology 12, 568–575. 10.1038/ni.2031. [PubMed: 21516111]

15. McGeachy MJ, Bak-Jensen KS, Chen Y, Tato CM, Blumenschein W, McClanahan T, and Cua DJ (2007). TGF-beta and IL-6 drive the production of IL-17 and IL-10 by T cells and restrain T(H)-17 cell-mediated pathology. Nature immunology 8, 1390–1397. 10.1038/ni1539. [PubMed: 17994024]
16. Leppkes M, Becker C, Ivanov II, Hirth S, Wirtz S, Neufert C, Pouly S, Murphy AJ, Valenzuela DM, Yancopoulos GD, et al. (2009). RORgamma-expressing Th17 cells induce murine chronic intestinal inflammation via redundant effects of IL-17A and IL-17F. Gastroenterology 136, 257–267. [PubMed: 18992745]
17. Alexander M, Ang QY, Nayak RR, Bustion AE, Sandy M, Zhang B, Upadhyay V, Pollard KS, Lynch SV, and Turnbaugh PJ (2022). Human gut bacterial metabolism drives Th17 activation and colitis. Cell host & microbe 30, 17–30 e19. 10.1016/j.chom.2021.11.001. [PubMed: 34822777]
18. Basu R, O'Quinn DB, Silberger DJ, Schoeb TR, Fouser L, Ouyang W, Hatton RD, and Weaver CT (2012). Th22 cells are an important source of IL-22 for host protection against enteropathogenic bacteria. Immunity 37, 1061–1075. 10.1016/j.immuni.2012.08.024. [PubMed: 23200827]
19. Maxwell JR, Zhang Y, Brown WA, Smith CL, Byrne FR, Fiorino M, Stevens E, Bigler J, Davis JA, Rottman JB, et al. (2015). Differential Roles for Interleukin-23 and Interleukin-17 in Intestinal Immunoregulation. Immunity 43, 739–750. 10.1016/j.immuni.2015.08.019. [PubMed: 26431947]
20. Lee JS, Tato CM, Joyce-Shaikh B, Gulen MF, Cayatte C, Chen Y, Blumenschein WM, Judo M, Ayanoglu G, McClanahan TK, et al. (2015). Interleukin-23-Independent IL-17 Production Regulates Intestinal Epithelial Permeability. Immunity 43, 727–738. 10.1016/j.immuni.2015.09.003. [PubMed: 26431948]
21. Fauny M, Moulin D, D'Amico F, Netter P, Petitpain N, Arnone D, Jouzeau JY, Loeuille D, and Peyrin-Biroulet L (2020). Paradoxical gastrointestinal effects of interleukin-17 blockers. Annals of the rheumatic diseases 79, 1132–1138. 10.1136/annrheumdis-2020-217927. [PubMed: 32719044]
22. Gagliani N, Amezcua Vesely MC, Iseppon A, Brockmann L, Xu H, Palm NW, de Zoete MR, Licona-Limon P, Paiva RS, Ching T, et al. (2015). Th17 cells transdifferentiate into regulatory T cells during resolution of inflammation. Nature 523, 221–225. 10.1038/nature14452. [PubMed: 25924064]
23. Schnell A, Littman DR, and Kuchroo VK (2023). T(H)17 cell heterogeneity and its role in tissue inflammation. Nature immunology 24, 19–29. 10.1038/s41590-022-01387-9. [PubMed: 36596896]
24. Omenetti S, Bussi C, Metidji A, Iseppon A, Lee S, Tolaini M, Li Y, Kelly G, Chakravarty P, Shoaie S, et al. (2019). The Intestine Harbors Functionally Distinct Homeostatic Tissue-Resident and Inflammatory Th17 Cells. Immunity 51, 77–89 e76. 10.1016/j.immuni.2019.05.004. [PubMed: 31229354]
25. Chihara N, Madi A, Kondo T, Zhang H, Acharya N, Singer M, Nyman J, Marjanovic ND, Kowalczyk MS, Wang C, et al. (2018). Induction and transcriptional regulation of the co-inhibitory gene module in T cells. Nature 558, 454–459. 10.1038/s41586-018-0206-z. [PubMed: 29899446]
26. Crawford A, Angelosanto JM, Kao C, Doering TA, Odorizzi PM, Barnett BE, and Wherry EJ (2014). Molecular and transcriptional basis of CD4(+) T cell dysfunction during chronic infection. Immunity 40, 289–302. 10.1016/j.immuni.2014.01.005. [PubMed: 24530057]
27. Martinez GJ, Pereira RM, Aijo T, Kim EY, Marangoni F, Pipkin ME, Togher S, Heissmeyer V, Zhang YC, Crotty S, et al. (2015). The transcription factor NFAT promotes exhaustion of activated CD8(+) T cells. Immunity 42, 265–278. 10.1016/j.immuni.2015.01.006. [PubMed: 25680272]
28. Alfei F, Kanev K, Hofmann M, Wu M, Ghoneim HE, Roelli P, Utzschneider DT, von Hoesslin M, Cullen JG, Fan Y, et al. (2019). TOX reinforces the phenotype and longevity of exhausted T cells in chronic viral infection. Nature 571, 265–269. 10.1038/s41586-019-1326-9. [PubMed: 31207605]
29. Aschenbrenner D, Foglierini M, Jarrossay D, Hu D, Weiner HL, Kuchroo VK, Lanzavecchia A, Notarbartolo S, and Sallusto F (2018). An immunoregulatory and tissue-residency program modulated by c-MAF in human TH17 cells. Nature immunology 19, 1126–1136. 10.1038/s41590-018-0200-5. [PubMed: 30201991]

30. Cao S, Liu J, Song L, and Ma X (2005). The protooncogene c-Maf is an essential transcription factor for IL-10 gene expression in macrophages. Journal of immunology 174, 3484–3492. 10.4049/jimmunol.174.6.3484.

31. Xu J, Yang Y, Qiu G, Lal G, Wu Z, Levy DE, Ochando JC, Bromberg JS, and Ding Y (2009). c-Maf regulates IL-10 expression during Th17 polarization. Journal of immunology 182, 6226–6236. 10.4049/jimmunol.0900123.

32. Pot C, Jin H, Awasthi A, Liu SM, Lai CY, Madan R, Sharpe AH, Karp CL, Miaw SC, Ho IC, and Kuchroo VK (2009). Cutting edge: IL-27 induces the transcription factor c-Maf, cytokine IL-21, and the costimulatory receptor ICOS that coordinately act together to promote differentiation of IL-10-producing Tr1 cells. Journal of immunology 183, 797–801. 10.4049/jimmunol.0901233.

33. Apetoh L, Quintana FJ, Pot C, Joller N, Xiao S, Kumar D, Burns EJ, Sherr DH, Weiner HL, and Kuchroo VK (2010). The aryl hydrocarbon receptor interacts with c-Maf to promote the differentiation of type 1 regulatory T cells induced by IL-27. Nature immunology 11, 854–861. 10.1038/ni.1912. [PubMed: 20676095]

34. Zhu C, Sakuishi K, Xiao S, Sun Z, Zaghouani S, Gu G, Wang C, Tan DJ, Wu C, Rangachari M, et al. (2015). An IL-27/NFIL3 signalling axis drives Tim-3 and IL-10 expression and T-cell dysfunction. Nat Commun 6, 6072. 10.1038/ncomms7072. [PubMed: 25614966]

35. Ridley ML, Fleskens V, Roberts CA, Lalnunhlimi S, Alnesf A, O'Byrne AM, Steel KJA, Povoleri GAM, Sumner J, Lavender P, and Taams LS (2020). IKZF3/Aiolos Is Associated with but Not Sufficient for the Expression of IL-10 by CD4(+) T Cells. Journal of immunology 204, 2940–2948. 10.4049/jimmunol.1901283.

36. Ciofani M, Madar A, Galan C, Sellars M, Mace K, Pauli F, Agarwal A, Huang W, Parkhurst CN, Muratet M, et al. (2012). A validated regulatory network for Th17 cell specification. Cell 151, 289–303. 10.1016/j.cell.2012.09.016. [PubMed: 23021777]

37. Tan TG, Sefik E, Geva-Zatorsky N, Kua L, Naskar D, Teng F, Pasman L, Ortiz-Lopez A, Jupp R, Wu HJ, et al. (2016). Identifying species of symbiont bacteria from the human gut that, alone, can induce intestinal Th17 cells in mice. Proceedings of the National Academy of Sciences of the United States of America 113, E8141–E8150. 10.1073/pnas.1617460113. [PubMed: 27911839]

38. Zuberbuehler MK, Parker ME, Wheaton JD, Espinosa JR, Salzler HR, Park E, and Ciofani M (2019). The transcription factor c-Maf is essential for the commitment of IL-17-producing gammadelta T cells. Nature immunology 20, 73–85. 10.1038/s41590-018-0274-0. [PubMed: 30538336]

39. Neumann C, Blume J, Roy U, Teh PP, Vasanthakumar A, Beller A, Liao Y, Heinrich F, Arenzana TL, Hackney JA, et al. (2019). c-Maf-dependent T(reg) cell control of intestinal T(H)17 cells and IgA establishes host-microbiota homeostasis. Nature immunology 20, 471–481. 10.1038/s41590-019-0316-2. [PubMed: 30778241]

40. Hu D, Notarbartolo S, Croonenborghs T, Patel B, Cialic R, Yang TH, Aschenbrenner D, Andersson KM, Gattorno M, Pham M, et al. (2017). Transcriptional signature of human pro-inflammatory T(H)17 cells identifies reduced IL10 gene expression in multiple sclerosis. Nat Commun 8, 1600. 10.1038/s41467-017-01571-8. [PubMed: 29150604]

41. Goto Y, Panea C, Nakato G, Cebula A, Lee C, Diez MG, Laufer TM, Ignatowicz L, and Ivanov II (2014). Segmented filamentous bacteria antigens presented by intestinal dendritic cells drive mucosal Th17 cell differentiation. Immunity 40, 594–607. 10.1016/j.immuni.2014.03.005. [PubMed: 24684957]

42. Farkas AM, Panea C, Goto Y, Nakato G, Galan-Diez M, Narushima S, Honda K, and Ivanov II (2015). Induction of Th17 cells by segmented filamentous bacteria in the murine intestine. J Immunol Methods 421, 104–111. 10.1016/j.jim.2015.03.020. [PubMed: 25858227]

43. Sano T, Huang W, Hall JA, Yang Y, Chen A, Gavzy SJ, Lee JY, Ziel JW, Miraldi ER, Domingos AI, et al. (2015). An IL-23R/IL-22 Circuit Regulates Epithelial Serum Amyloid A to Promote Local Effector Th17 Responses. Cell 163, 381–393. 10.1016/j.cell.2015.08.061. [PubMed: 26411290]

44. Stenstad H, Ericsson A, Johansson-Lindbom B, Svensson M, Marsal J, Mack M, Picarella D, Soler D, Marquez G, Briskin M, and Agace WW (2006). Gut-associated lymphoid tissue-primed CD4+ T cells display CCR9-dependent and -independent homing to the small intestine. Blood 107, 3447–3454. 10.1182/blood-2005-07-2860. [PubMed: 16391017]

45. Woodward Davis AS, Roozen HN, Dufort MJ, DeBerg HA, Delaney MA, Mair F, Erickson JR, Slichter CK, Berkson JD, Klock AM, et al. (2019). The human tissue-resident CCR5(+) T cell compartment maintains protective and functional properties during inflammation. Sci Transl Med 11. 10.1126/scitranslmed.aaw8718.
46. Iijima N, and Iwasaki A (2014). T cell memory. A local macrophage chemokine network sustains protective tissue-resident memory CD4 T cells. Science 346, 93–98. 10.1126/science.1257530. [PubMed: 25170048]
47. Turner DL, and Farber DL (2014). Mucosal resident memory CD4 T cells in protection and immunopathology. Front Immunol 5, 331. 10.3389/fimmu.2014.00331. [PubMed: 25071787]
48. Wagner A, Wang C, Fessler J, DeTomaso D, Avila-Pacheco J, Kaminski J, Zaghouani S, Christian E, Thakore P, Schellhaass B, et al. (2021). Metabolic modeling of single Th17 cells reveals regulators of autoimmunity. Cell 184, 4168–4185 e4121. 10.1016/j.cell.2021.05.045. [PubMed: 34216539]
49. Schnell A, Huang L, Singer M, Singaraju A, Barilla RM, Regan BML, Bollhagen A, Thakore PI, Dionne D, Delorey TM, et al. (2021). Stem-like intestinal Th17 cells give rise to pathogenic effector T cells during autoimmunity. Cell 184, 6281–6298 e6223. 10.1016/j.cell.2021.11.018. [PubMed: 34875227]
50. Nish SA, Zens KD, Kratchmarov R, Lin WW, Adams WC, Chen YH, Yen B, Rothman NJ, Bhandoola A, Xue HH, et al. (2017). CD4+ T cell effector commitment coupled to self-renewal by asymmetric cell divisions. The Journal of experimental medicine 214, 39–47. 10.1084/jem.20161046. [PubMed: 27923906]
51. Groux H, O'Garra A, Bigler M, Rouleau M, Antonenko S, de Vries JE, and Roncarolo MG (1997). A CD4+ T-cell subset inhibits antigen-specific T-cell responses and prevents colitis. Nature 389, 737–742. 10.1038/39614. [PubMed: 9338786]
52. Brockmann L, Gagliani N, Steglich B, Giannou AD, Kempski J, Pelczar P, Geffken M, Mfarrej B, Huber F, Herkel J, et al. (2017). IL-10 Receptor Signaling Is Essential for TR1 Cell Function In Vivo. Journal of immunology 198, 1130–1141. 10.4049/jimmunol.1601045.
53. Chaudhry A, Samstein RM, Treuting P, Liang Y, Pils MC, Heinrich JM, Jack RS, Wunderlich FT, Bruning JC, Muller W, and Rudensky AY (2011). Interleukin-10 signaling in regulatory T cells is required for suppression of Th17 cell-mediated inflammation. Immunity 34, 566–578. 10.1016/j.immuni.2011.03.018. [PubMed: 21511185]
54. Panea C, Farkas AM, Goto Y, Abdollahi-Roodsaz S, Lee C, Koscsó B, Gowda K, Hohl TM, Bogunovic M, and Ivanov II (2015). Intestinal Monocyte-Derived Macrophages Control Commensal-Specific Th17 Responses. Cell Reports 12, 1314–1324. 10.1016/j.celrep.2015.07.040. [PubMed: 26279572]
55. Zigmond E, Bernshtein B, Friedlander G, Walker CR, Yona S, Kim KW, Brenner O, Krauthgamer R, Varol C, Muller W, and Jung S (2014). Macrophage-restricted interleukin-10 receptor deficiency, but not IL-10 deficiency, causes severe spontaneous colitis. Immunity 40, 720–733. 10.1016/j.immuni.2014.03.012. [PubMed: 24792913]
56. Shih VF, Cox J, Kljavin NM, Dengler HS, Reichelt M, Kumar P, Rangell L, Kolls JK, Diehl L, Ouyang W, and Ghilardi N (2014). Homeostatic IL-23 receptor signaling limits Th17 response through IL-22-mediated containment of commensal microbiota. Proceedings of the National Academy of Sciences of the United States of America 111, 13942–13947. 10.1073/pnas.1323852111. [PubMed: 25201978]
57. Kawano Y, Edwards M, Huang Y, Bilate AM, Araujo LP, Tanoue T, Atarashi K, Ladinsky MS, Reiner SL, Wang HH, et al. (2022). Microbiota imbalance induced by dietary sugar disrupts immune-mediated protection from metabolic syndrome. Cell 185, 3501–3519 e3520. 10.1016/j.cell.2022.08.005. [PubMed: 36041436]
58. Xu M, Pokrovskii M, Ding Y, Yi R, Au C, Harrison OJ, Galan C, Belkaid Y, Bonneau R, and Littman DR (2018). c-MAF-dependent regulatory T cells mediate immunological tolerance to a gut pathobiont. Nature 554, 373–377. 10.1038/nature25500. [PubMed: 29414937]
59. Wheaton JD, Yeh CH, and Ciofani M (2017). Cutting Edge: c-Maf Is Required for Regulatory T Cells To Adopt RORgammat(+) and Follicular Phenotypes. Journal of immunology 199, 3931–3936. 10.4049/jimmunol.1701134.

60. Ladinsky MS, Araujo LP, Zhang X, Veltri J, Galan-Diez M, Soualhi S, Lee C, Irie K, Pinker EY, Narushima S, et al. (2019). Endocytosis of commensal antigens by intestinal epithelial cells regulates mucosal T cell homeostasis. Science 363. 10.1126/science.aat4042.

61. Xia Y, Sandor K, Pai JA, Daniel B, Raju S, Wu R, Hsiung S, Qi Y, Yangdon T, Okamoto M, et al. (2022). BCL6-dependent TCF-1(+) progenitor cells maintain effector and helper CD4(+) T cell responses to persistent antigen. Immunity 55, 1200–1215 e1206. 10.1016/j.immuni.2022.05.003. [PubMed: 35637103]

62. Utzschneider DT, Charmoy M, Chennupati V, Pousse L, Ferreira DP, Calderon-Copete S, Danilo M, Alfei F, Hofmann M, Wieland D, et al. (2016). T Cell Factor 1-Expressing Memory-like CD8(+) T Cells Sustain the Immune Response to Chronic Viral Infections. Immunity 45, 415–427. 10.1016/j.immuni.2016.07.021. [PubMed: 27533016]

63. Kamanaka M, Huber S, Zenewicz LA, Gagliani N, Rathinam C, O'Connor W Jr., Wan YY, Nakae S, Iwakura Y, Hao L, and Flavell RA (2011). Memory/effector (CD45RB(lo)) CD4 T cells are controlled directly by IL-10 and cause IL-22-dependent intestinal pathology. The Journal of experimental medicine 208, 1027–1040. 10.1084/jem.20102149. [PubMed: 21518800]

64. Kamanaka M, Kim ST, Wan YY, Sutterwala FS, Lara-Tejero M, Galan JE, Harhaj E, and Flavell RA (2006). Expression of interleukin-10 in intestinal lymphocytes detected by an interleukin-10 reporter knockin tiger mouse. Immunity 25, 941–952. 10.1016/j.immuni.2006.09.013. [PubMed: 17137799]

65. Hohl TM, Rivera A, Lipuma L, Gallegos A, Shi C, Mack M, and Pamer EG (2009). Inflammatory monocytes facilitate adaptive CD4 T cell responses during respiratory fungal infection. Cell host & microbe 6, 470–481. 10.1016/j.chom.2009.10.007. [PubMed: 19917501]

66. Roers A, Siewe L, Strittmatter E, Deckert M, Schluter D, Stenzel W, Gruber AD, Krieg T, Rajewsky K, and Muller W (2004). T cell-specific inactivation of the interleukin 10 gene in mice results in enhanced T cell responses but normal innate responses to lipopolysaccharide or skin irritation. The Journal of experimental medicine 200, 1289–1297. 10.1084/jem.20041789. [PubMed: 15534372]

67. DeTomaso D, Jones MG, Subramaniam M, Ashuach T, Ye CJ, and Yosef N (2019). Functional interpretation of single cell similarity maps. Nat Commun 10, 4376. 10.1038/s41467-019-12235-0. [PubMed: 31558714]

68. Delaney C, Schnell A, Cammarata LV, Yao-Smith A, Regev A, Kuchroo VK, and Singer M (2019). Combinatorial prediction of marker panels from single-cell transcriptomic data. Mol Syst Biol 15, e9005. 10.15252/msb.20199005. [PubMed: 31657111]

69. Street K, Risso D, Fletcher RB, Das D, Ngai J, Yosef N, Purdom E, and Dudoit S (2018). Slingshot: cell lineage and pseudotime inference for single-cell transcriptomics. BMC Genomics 19, 477. 10.1186/s12864-018-4772-0. [PubMed: 29914354]

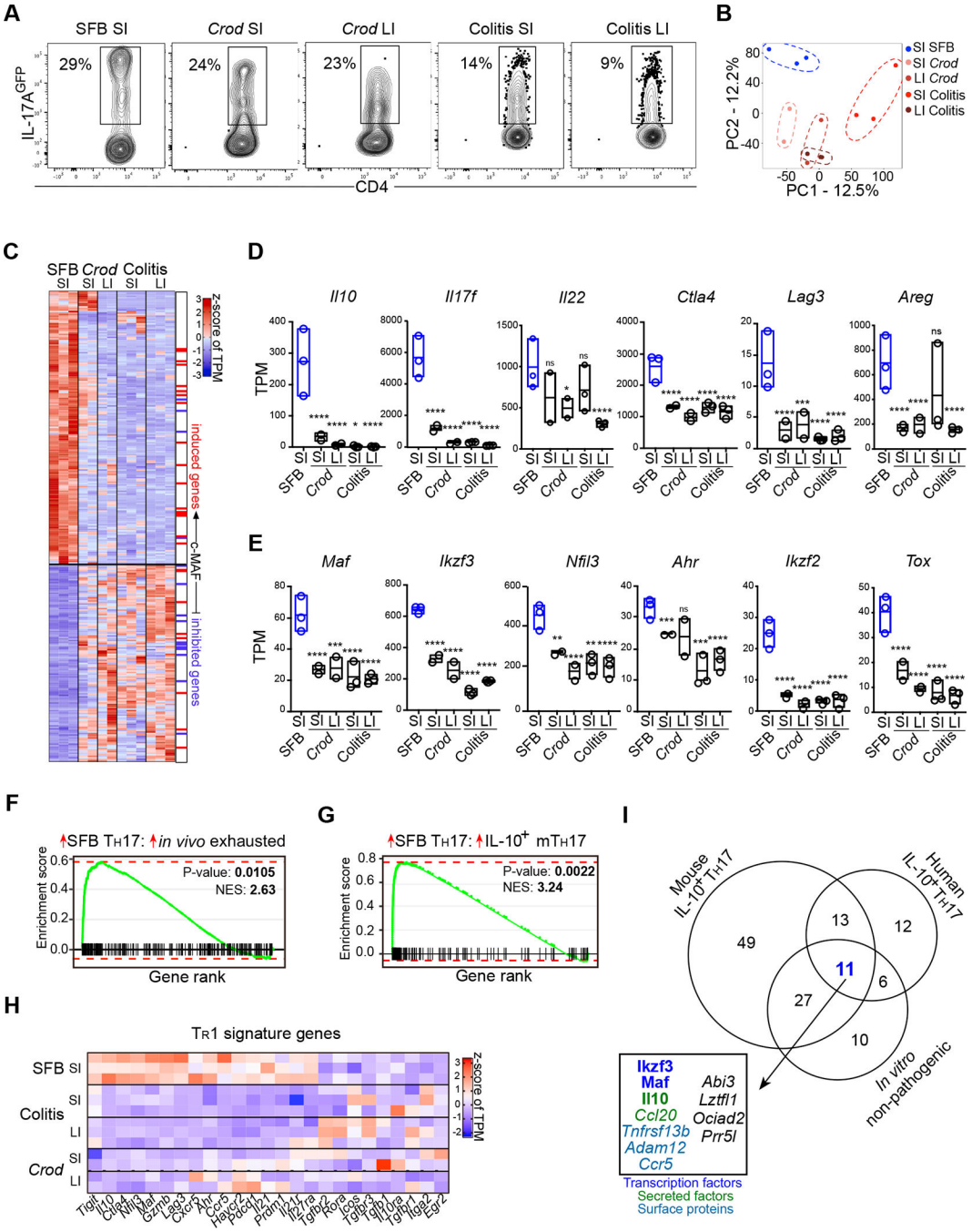

Figure 1. SFB T_H17 cells have an anti-inflammatory transcriptional program

(A) Intestinal lamina propria (LP) T_H17 cells induced by various mechanisms. SI, small intestine; LI, large intestine; Colitis, $CD45RB^{hi}$ colitis. Representative FACS plots gated on $TCR\beta^+CD4^+$ LP lymphocytes.

(B) PCA plot of RNA-sequencing analysis of various intestinal LP T_H17 cells. One experiment, *N*=2–3 mice/group.

(C) Heatmap of core SFB T_H17 cells program genes in bulk RNA-seq samples from (B). c-MAF controlled genes[36] are also marked on the right.

(D) Expression of selected cytokines and inhibitory receptors in LP T_H17 cells in RNA-Seq data from (B).

(E) Expression of selected transcription factors in LP T_H17 cells in RNA-Seq data from (B).

(F) Gene set enrichment analysis (GSEA) of genes upregulated in SFB T_H17 cells compared to genes upregulated in exhausted CD4 T cells[26].

(G) GSEA of genes upregulated in SFB T_H17 cells compared to genes upregulated in mouse IL-10^+ T_H17 cells[12].

(H) Expression of T_R1 signature genes in various intestinal LP T_H17 cells.

(I) Venn Diagram of leading-edge genes from GSEA of genes upregulated in SFB T_H17 cells and published datasets[12,13,29].

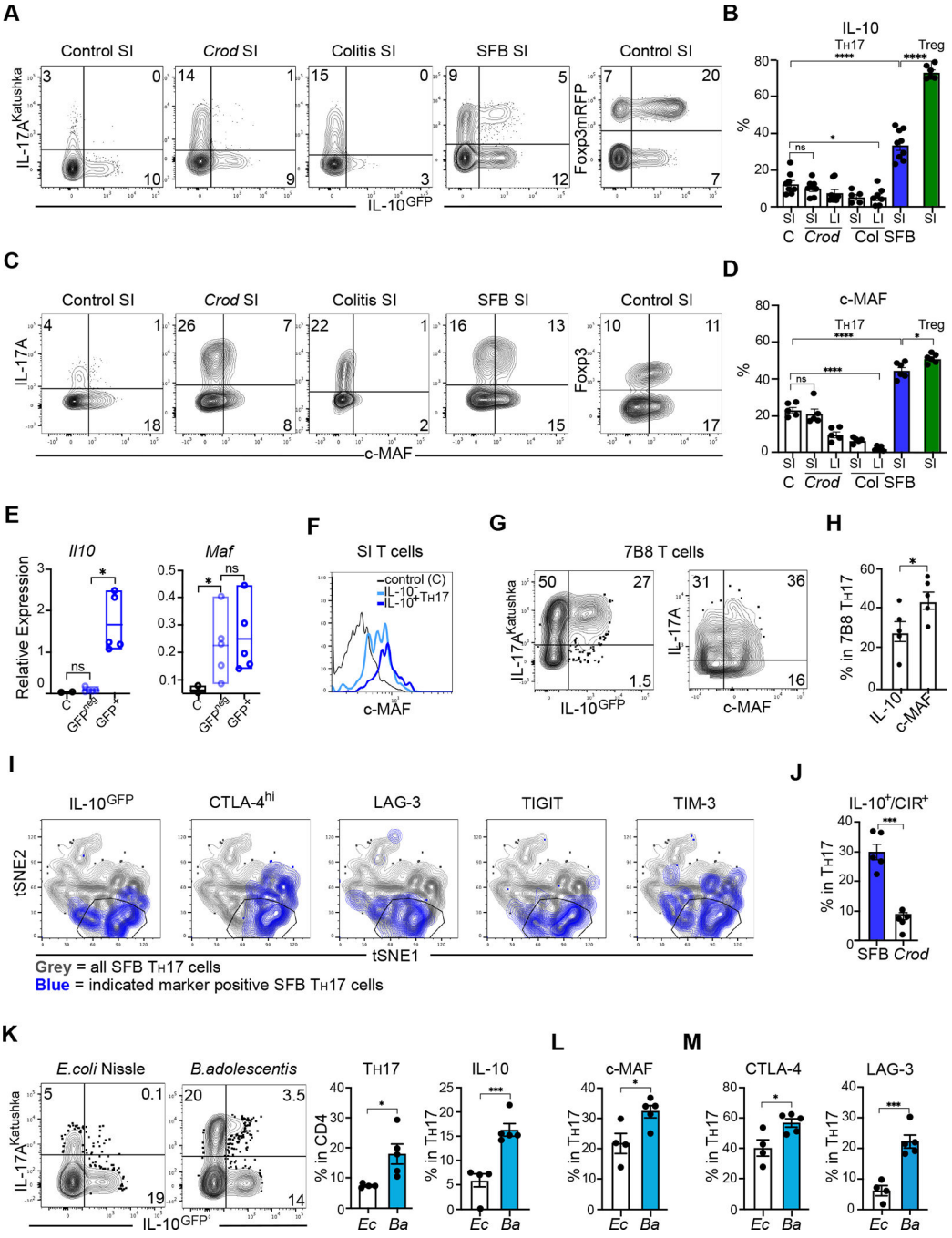

Figure 2. SFB T_H17 cells express IL-10 and co-inhibitory receptors

(A, B) IL-10 expression in SI LP T_H17 cells and Foxp3$^+$ Tregs from *Il10^{GFP}/Il17a^{Katushka}/Foxp3^{mRFP}* mice under various conditions. IL-17/IL-10 FACS plots in (A) gated on TCRβ$^+$CD4$^+$Foxp3^{mRFPneg} lymphocytes. Foxp3/IL-10 FACS plot in (A) gated on TCRβ$^+$CD4$^+$IL-17^{Katushkaneg} lymphocytes. (B) IL-10 (GFP) expression in T_H17 (TCRβ$^+$CD4$^+$Foxp3^{mRFPneg}IL-17$^{Katushka+}$) or Treg (TCRβ$^+$CD4$^+$Foxp3^{mRFP+}) cells. Three independent experiments, *N*=5–9 mice/group.

(C, D) c-MAF expression (intracellular staining) in SI LP T_H17 cells and Foxp3$^+$ Tregs. FACS plots in (C) gated on TCRβ$^+$CD4$^+$ LP lymphocytes. (D) c-MAF expression in T_H17 (TCRβ$^+$CD4$^+$IL-17$^+$) or Treg (TCRβ$^+$CD4$^+$Foxp3$^+$) cells. Two independent experiments, *N*=5–6 mice/group.

(E) qPCR of *Il10* and *Maf* transcripts in IL-10^{GFPneg} and IL-10^{GFP+} SFB T_H17 cells (TCRβ$^+$CD4$^+$Foxp3^{mRFPneg}IL-17$^{Katushka+}$) and IL-10^{GFPneg}/IL-17^{Katushkaneg}/Foxp3^{mRFPneg} control (C) CD4 T cells FACS-purified from SI LP of *Il10^{GFP}/Il17a^{Katushka}/Foxp3^{mRFP}* mice. Two independent experiments, *N*=2–5 mice/group.

(F) Representative histograms of c-MAF expression (intracellular staining) in IL-10^{GFPneg} and IL-10^{GFP+} T_H17 cells and control CD4 T cells FACS-purified from SI LP of SFB-colonized *Il10^{GFP}*/*Il17a^{Katushka}*/*Foxp3^{mRFP}* mice. Two independent experiments, *N*=2–5 mice/group.

(G, H) Naive 7B8 SFB-specific TCR Tg CD4 T cells from 7B8 *Il10^{GFP}/Il17a^{Katushka}/Foxp3^{mRFP}* mice were adoptively transferred into SFB-colonized congenic wild type mice. IL-10 (GFP) and c-MAF (intracellular staining) expression in transferred CD4 T cells was examined one week later. FACS plots gated on Ly5.1$^+$CD4$^+$TCRβ$^+$Foxp3^{neg} transferred 7B8 cells. Bar plots further gated on IL-17$^+$ T_H17 cells. Two independent experiments, *N*=5 mice.

(I, J) tSNE analysis based on multi-parameter flow cytometry of IL-10 and co-inhibitory receptors (CIR) expression in SI LP T_H17 cells from SFB-colonized (I, J) or *Citrobacter rodentium* (*Crod*) infected (J) *Il10^{GFP}/Il17a^{Katushka}/Foxp3^{mRFP}* mice. Plots gated on Ly5.1$^+$CD4$^+$TCRβ$^+$Foxp3^{mRFPneg}IL-17$^{Katushka+}$ cells. Two independent experiments, *N*=5 mice/group.

(K) T_H17 cell induction and IL-10 expression in SI LP T_H17 cells from *Il10^{GFP}/Il17a^{Katushka}/Foxp3^{mRFP}* mice after oral gavage of *E. coli* (*Ec*) or *B. adolescentis* (*Ba*) every other day for two weeks. IL-17/IL-10 FACS plots gated on TCRβ$^+$CD4$^+$Foxp3^{mRFPneg} lymphocytes. Two independent experiments, *N*=4–5 mice/group.

(L, M) c-MAF (intracellular staining) (L) and LAG-3 and CTLA-4 expression (M) in SI LP T_H17 cells the experiments in (K). Two independent experiments, *N*=4–5 mice/group.

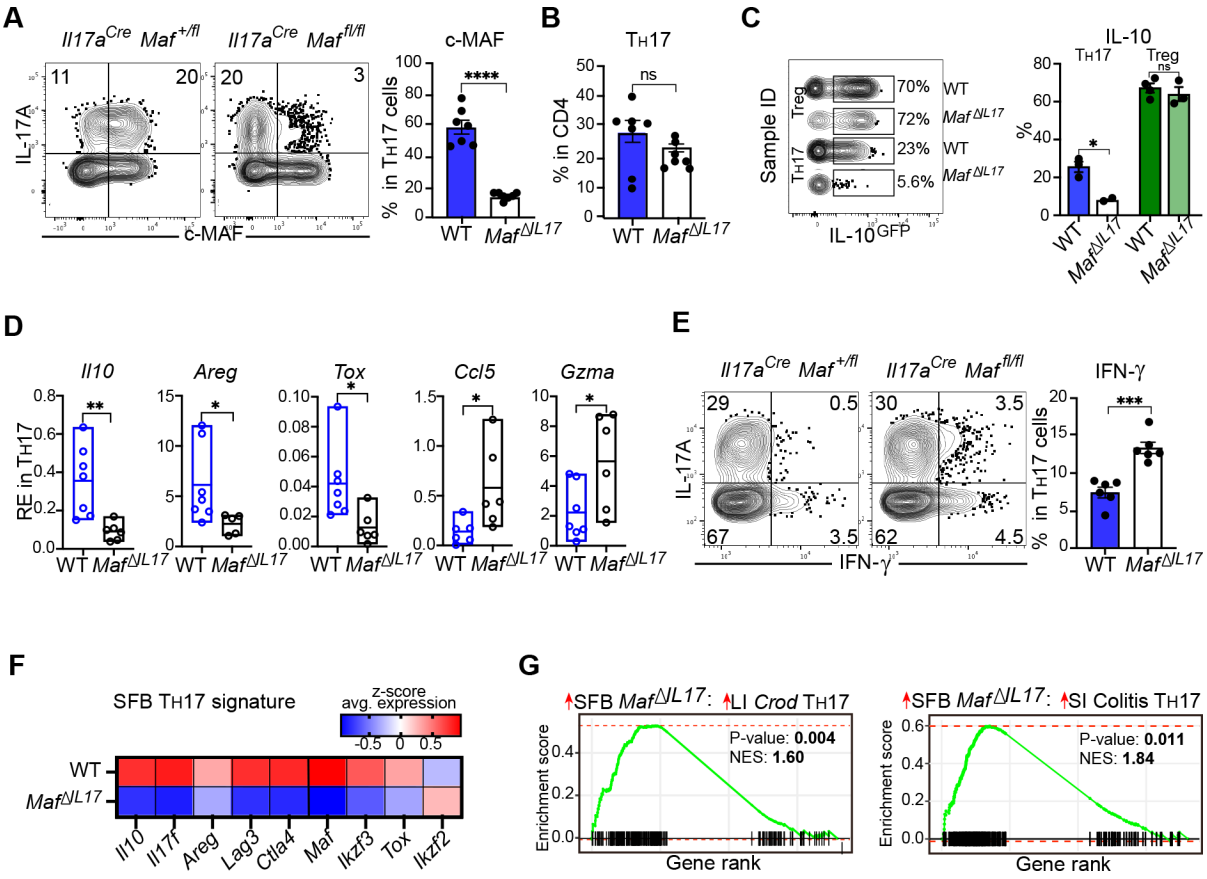

Figure 3. c-MAF drives anti-inflammatory identity of intestinal commensal T_H17 cells

(A) Intracellular staining for c-MAF in CD4 T (TCRβ$^+$CD4$^+$Foxp3^{mRFPneg}) and T_H17 (TCRβ$^+$CD4$^+$IL-17$^+$) cells from SI LP of *Foxp3^{mRFP}/R26$^{STOP\text{-}YFP}$/Il17a^{Cre}/Maf$^{flox/flox}$* (*Maf^{ΔIL17}*) mice and *Foxp3^{mRFP}/R26$^{STOP\text{-}YFP}$/Il17a^{Cre}/Maf$^{flox/+}$* (WT) littermates. Three independent experiments, *N*=5–7 mice/group.

(B) Frequency of T_H17 cells (intracellular staining) in SI LP of WT and *Maf^{ΔIL17}* mice. Three independent experiments, *N*=7 mice/group.

(C) IL-10^{GFP} expression in SI LP T_H17 cells and Foxp3$^+$ Tregs from *Il10^{GFP}/Il17a^{Katushka}/Foxp3^{mRFP}/R26$^{STOP\text{-}YFP}$/Il17a^{Cre}/Maf$^{flox/flox}$* (*Maf^{ΔIL17}*) and littermate control (WT) mice. FACS plots gated on TCRβ$^+$CD4$^+$Foxp3^{mRFPneg}IL-17$^{Katushka+}$ (T_H17) or TCRβ$^+$CD4$^+$Foxp3^{mRFP+} (Treg) lymphocytes. Two independent experiments, *N*=2–4 mice/group

(D) Quantitative PCR of *Il10, Areg, Tox, Ccl5* and *Gzma* mRNA in FACS-purified SI LP TH17 cells (TCRβ$^+$CD4$^+$Foxp3^{mRFPneg}IL-17$^{Katushka+}$) from WT and *Maf^{ΔIL17}* (*Il10^{GFP}/Il17a^{Katushka}/Foxp3^{mRFP}/R26$^{STOP\text{-}YFP}$/Il17a^{Cre}/Maf$^{flox/flox}$*) mice. Two independent experiments, *N*=6–7 mice/group.

(E) Intracellular staining for IL-17 and IFN-γ in (Left) CD4 T (TCRβ$^+$CD4$^+$) and (Right) T_H17 (TCRβ$^+$CD4$^+$IL-17$^+$) cells from SI LP of WT and *Maf^{ΔIL17}* (*Foxp3^{mRFP}/R26$^{STOP\text{-}YFP}$/Il17a^{Cre}/Maf$^{flox/flox}$*) mice. Two independent experiments, *N*=6 mice/group.

(F) Heatmap of selected SFB T_H17 cell signature genes in scRNA-Seq of FACS-purified SI LP T_H17 cells ($TCR\beta^+CD4^+Foxp3^{mRFPneg}IL\text{-}17^{YFP+}$) from WT and *Maf*$^{\Delta IL17}$ (*Foxp3*^{mRFP}/*R26*$^{STOP\text{-}YFP}$/*Il17a*^{Cre}/*Maf*$^{flox/flox}$) mice. One experiment, *N*=2–3 mice/group.

(G) GSEA of top 200 upregulated genes in *Maf*$^{\Delta IL17}$ SI LP SFB T_H17 cells ($TCR\beta^+CD4^+Foxp3^{mRFPneg}IL\text{-}17^{YFP+}$) compared to genes upregulated in LI *Crod* T_H17 cells and colitis T_H17 cells in bulk RNA-Seq datasets in Figure 1.

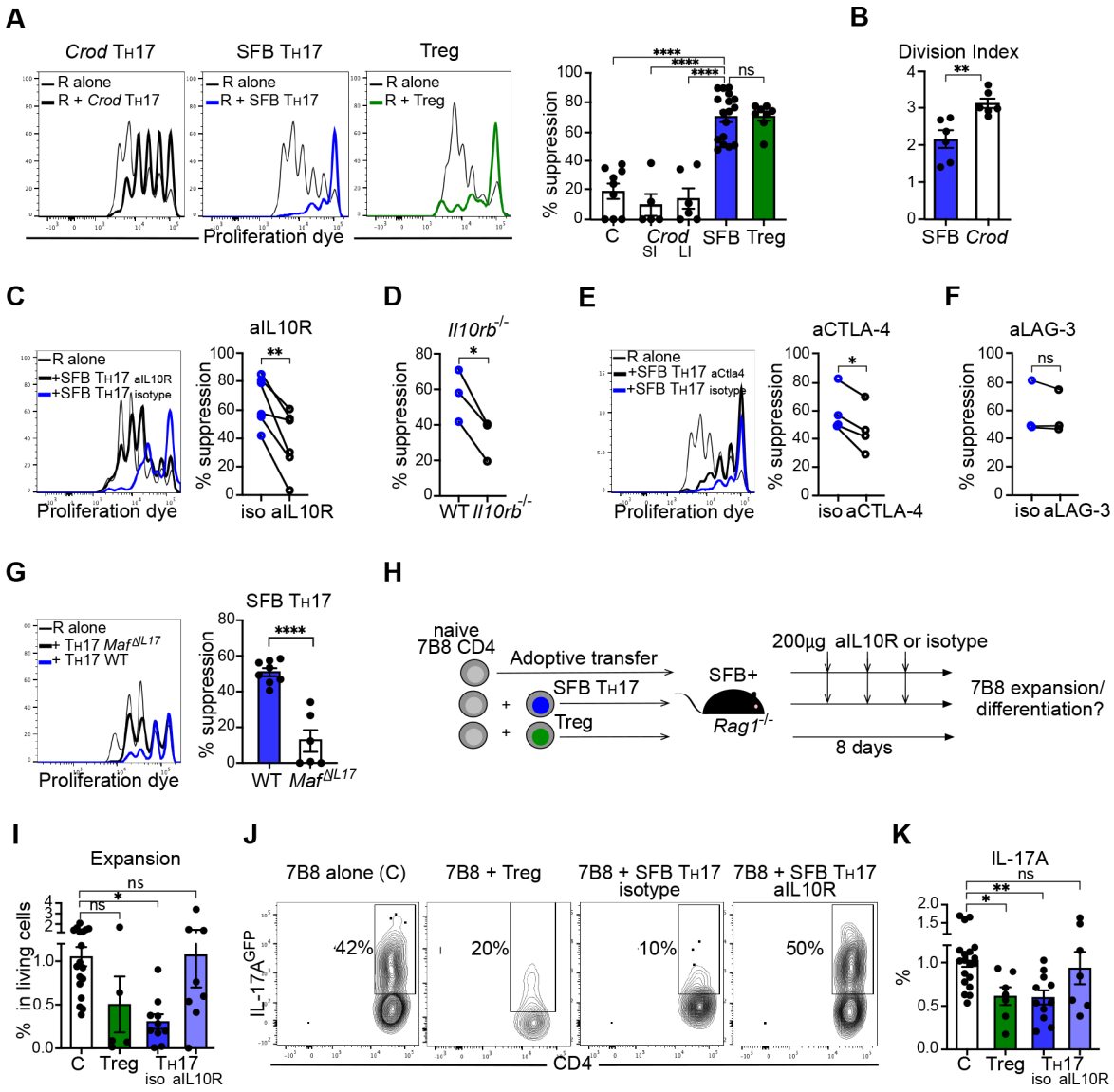

Figure 4. Regulatory functions of commensal T_H17 cells

(A) ***In vitro*** suppression assay. FACS-purified SI LP T_H17 cells (TCRβ$^+$CD4$^+$ Foxp3^{mRFPneg}IL-17^{GFP+}) from SFB-colonized or *Citrobacter rodentium* infected (*Crod*) mice or Treg cells (TCRβ$^+$CD4$^+$Foxp3^{mRFP+}) were co-cultured with WT naïve responder CD4 T cells from spleen of untreated mice as described in Methods. (Left) Proliferation of CTV-stained responder T cells (R) on Day 4. (Right) Percent suppression calculated as described in Methods. Cumulative of at least four independent experiments, *N*=2–3 technical replicates/experiment. Each dot represents a technical replicate.

(B) Division index (see Methods) of CTV-labelled SFB and *Crod* LP T_H17 cells in *in vitro* suppression assay. One experiment, *N*=3 mice/group and 2 technical replicates/mouse. Each dot represents a technical replicate.

(C) Proliferation of WT responder CD4 T cells (R) alone or co-cultured with FACS-purified SI LP SFB T_H17 cells (TCRβ$^+$CD4$^+$ Foxp3^{mRFPneg}IL-17^{GFP+}) in the presence of blocking

anti-IL-10R antibody or isotype control. Five independent experiments, *N*=2–3 technical replicates/experiment. Significance, paired t-test.

(D) Inhibition of proliferation of WT or *Il10rb*$^{-/-}$ responder CD4 T cells by purified WT SI LP SFB T_H17 cells (TCRβ$^+$CD4$^+$ Foxp3^{mRFPneg}IL-17^{GFP+}). Three independent experiments, *N*=2–3 technical replicates/experiment. Significance, paired t-test.

(E) Proliferation of WT responder CD4 T cells (R) alone or co-cultured with FACS-purified SI LP SFB T_H17 cells (TCRβ$^+$CD4$^+$ Foxp3^{mRFPneg}IL-17^{GFP+}) in the presence of blocking anti-CTLA-4 antibody or isotype control. Four independent experiments, *N*=2–3 technical replicates/experiment. Significance, paired t-test.

(F) Proliferation of WT responder CD4 T cells (R) alone or co-cultured with FACS-purified SI LP SFB T_H17 cells (TCRβ$^+$CD4$^+$ Foxp3^{mRFPneg}IL-17^{GFP+}) in the presence of blocking anti-LAG3 antibody or isotype control. Three independent experiments, 2–3 technical replicates/experiment. Significance, paired t-test.

(G) Proliferation of WT responder CD4 T cells (R) alone or co-cultured with SI LP SFB T_H17 cells (TCRβ$^+$CD4$^+$Foxp3^{mRFPneg}IL-17^{YFP+}) from WT or *Maf*$^{\Delta IL17}$ mice. Cumulative of three independent experiments, *N*=2–3 technical replicates/experiment. Each datapoint represents a technical replicate.

(H) Experimental schematic of *in vivo* suppression assay.

(I-K) Expansion (I) and T_H17 cell differentiation (J, K) of naïve 7B8 CD4 T cells (Ly5.1$^+$) in SI LP 8 days after transfer into SFB colonized RAG1-deficient mice alone (C) or with co-transfer of SI LP Treg cells (TCRβ$^+$CD4$^+$Foxp3^{mRFP+}) or SI LP SFB T_H17 cells (TCRβ$^+$CD4$^+$IL-17^{GFP+}) with and without neutralization of IL-10 signaling by intraperitoneal injection of an anti-IL-10R or isotype control antibody. (I, J, K) Plots gated on Ly5.1$^+$TCRβ$^+$CD4$^+$ (7B8) SI LP lymphocytes. (I, K) Data was normalized to the average of the corresponding control group. Cumulative of six independent experiments, *N*=7–17 mice/group.

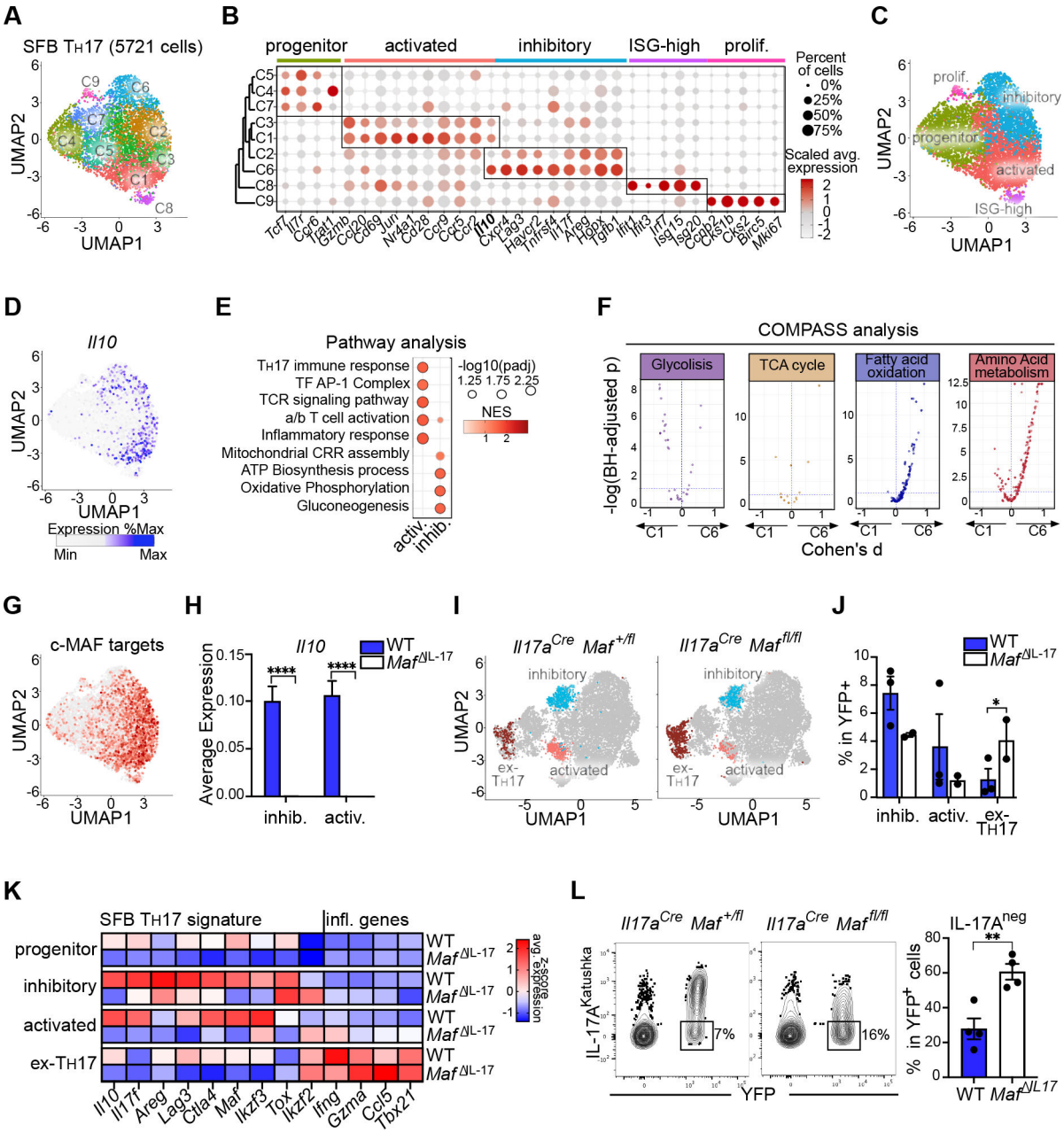

Figure 5. Commensal T_H17 cells are heterogeneous and contain two IL-10$^+$ populations

(A) UMAP clustering following scRNA-sequencing of 5721 SFB SI LP T_H17 cells (TCRβ$^+$CD4$^+$Foxp3^{mRFPneg}IL-17$^{Katushka+}$) sorted from *Il10^{GFP}/Il17a^{Katushka}/Foxp3^{mRFP}* reporter mice.

(B) Functional grouping of SI LP T_H17 cell clusters in (A) based on expression of select marker genes.

(C) UMAP with annotation of the functional groups in (B).

(D) Expression of *Il10* in individual SFB SI LP T_H17 cells overlayed over the UMAP clustering in (A).

(E) Pathway analysis of differentially expressed genes between activated and inhibitory IL-10^{+} expressing groups.

(F) COMPASS analysis for metabolic pathways in the two most differentiated IL-10^{+} UMAP clusters – C1 and C6.

(G) GSEA for c-MAF target genes[36] in individual SFB SI LP T_H17 cells overlayed over the UMAP clustering in (A).

(H) Expression of *Il10* mRNA in indicated functional groups in SI LP SFB T_H17 cells from WT (*Foxp3*^{mRFP}/*R26*$^{STOP\text{-}YFP}$/*Il17a*^{Cre}/*Maf*$^{flox/+}$) and *Maf*$^{\Delta IL17}$ (*Foxp3*^{mRFP}/*R26*$^{STOP\text{-}YFP}$/*Il17a*^{Cre}/*Maf*$^{flox/flox}$) mice, based on scRNA-Seq of SI LP T_H17 cells sorted based on YFP expression. Based on the functional clustering in Figure S5B. SI LP SFB T_H17 cells from individual mice were identified by hash-tagging of scRNA-Seq samples. *N*=2–3 mice/group.

(I) Frequency of cells in clusters C7 (ex- T_H17), C8 (inhibitory), and C10 (activated) based on the UMPA clustering in Figure S5A. Data from hash-tagged scRNA-Seq samples from WT and *Maf*$^{\Delta IL17}$ (*Foxp3*^{mRFP}/*R26*$^{STOP\text{-}YFP}$/*Il17a*^{Cre}/*Maf*$^{flox/flox}$) mice. Data integrated from *N*=2–3 mice/group.

(J) Statistics of (I)

(K) Heatmap of z score of average expression of selected SFB T_H17 signature genes and inflammatory genes in indicated functional groups based on UMAP in Figure S5B in hash-tagged scRNA-Seq samples from WT and *Maf*$^{\Delta IL17}$ (*Foxp3*^{mRFP}/*R26*$^{STOP\text{-}YFP}$/*Il17a*^{Cre}/*Maf*$^{flox/flox}$) mice.

(L) IL-17^{Katushka} and ROSA^{YFP} expression in (Left) CD4 T (TCRβ^{+}CD4^{+}Foxp3mRFPneg) and (Right) ex-T_H17 (TCRβ^{+}CD4^{+}IL-17^{YFP+}IL-17^{Katushkaneg}) cells from SI LP of WT and *Maf*$^{\Delta IL17}$ *Il10*^{GFP}/*Il17a*^{Katushka}*Foxp3*^{mRFP}/*R26*$^{STOP\text{-}YFP}$/*Il17a*^{Cre}/*Maf*$^{flox/flox}$ mice. *N*= 4 mice/group.

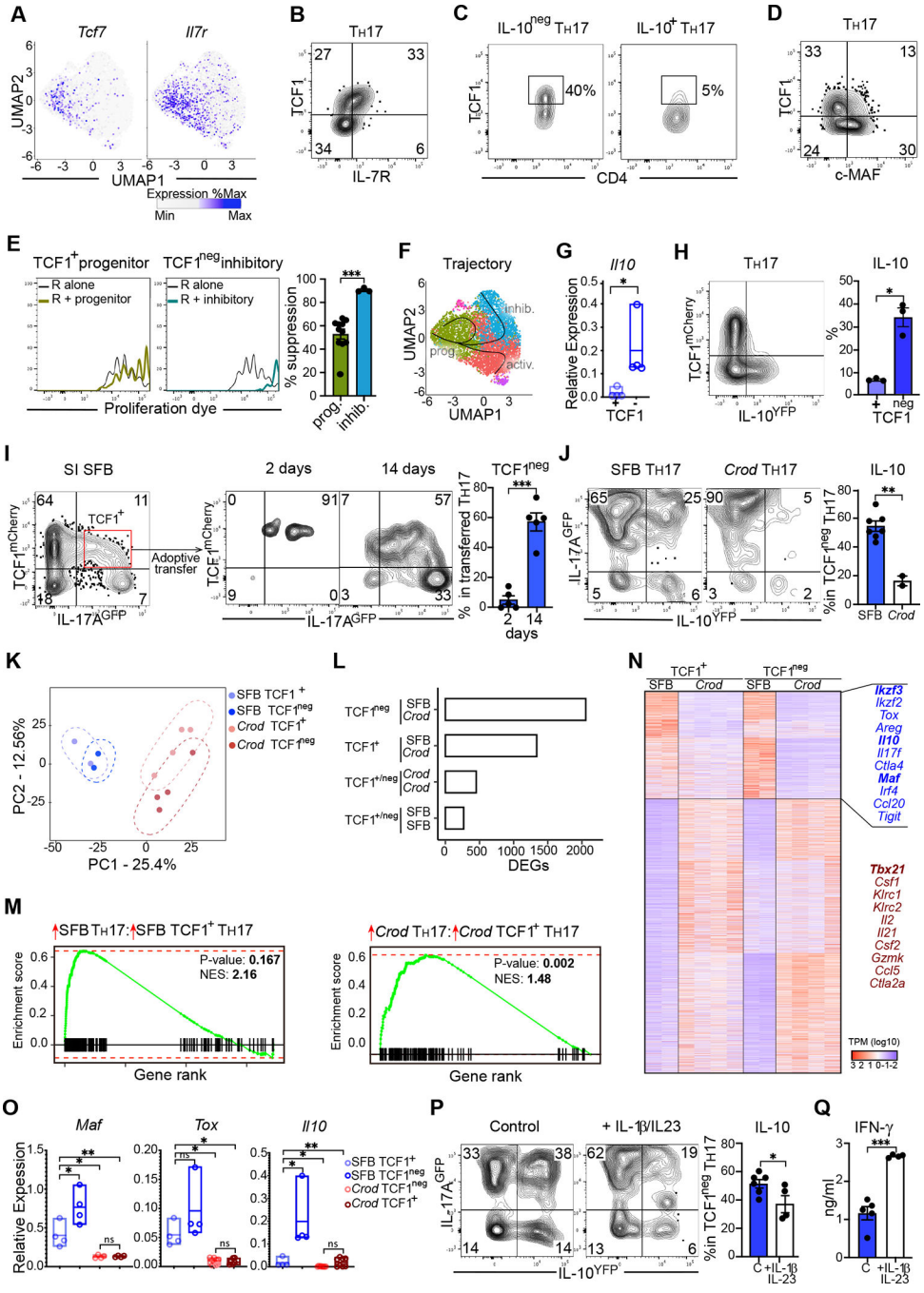

Figure 6. Commensal T_H17 cells contain a progenitor TCF1$^+$ population

(A) Expression of *Tcf7* and *Il7r* mRNA in individual SFB SI LP T_H17 cells overlayed over the UMAP clustering in Figure 5A.

(B) TCF1 and IL-7R expression in SI LP SFB T_H17 cells. Gated on TCRβ$^+$CD4$^+$IL-17$^+$ lymphocytes.

(C) Intracellular staining for TCF1 in FACS-purified IL-10^{GFPneg} and IL-10^{GFP+} SI LP SFB TH17 cells (TCRβ$^+$CD4$^+$Foxp3^{mRFPneg}IL-17$^{Katushka+}$).

(D) Intracellular staining for TCF1 and c-MAF in SI LP SFB T_H17 cells. Gated on TCRβ$^+$CD4$^+$IL-17$^+$ lymphocytes.

(E) FACS-purified SI LP SFB progenitor T_H17 cells (TCRβ$^+$CD4$^+$Foxp3^{mRFPneg}IL-17$^{Katushka+}$IL-10^{GFPneg}IL-7R$^+$) and SI LP SFB inhibitory T_H17 cells (TCRβ$^+$CD4$^+$Foxp3^{mRFPneg}IL-17$^{Katushka+}$IL-10^{GFP+}LAG-3$^+$) were co-cultured with WT naïve responder CD4 T cells. (Left) Proliferation of CTV-stained responder T cells (R) on Day 4. (Right) Percent suppression. Cumulative of three independent experiments. Each dot represents a technical replicate.

(F) Trajectory analysis of scRNA-Seq data in Figure 5A with a start node in C4. UMAP annotation as in Figure 5C.

(G) Quantitative PCR for *Il10* mRNA in FACS-purified TCF1$^{mCherry+}$ and TCF1^{mCherryneg} SI LP SFB T_H17 cells from *Tcf7*^{mCherry}/*Il17a*^{GFP} mice. Two independent experiments, *N*=4 mice/group.

(H) TCF1^{mCherry} and IL-10^{Venus} expression in SI LP SFB T_H17 cells (TCRβ$^+$CD4$^+$IL-17^{GFP+}) from *Tcf7*^{mCherry}/*Il17a*^{GFP}/*Il10*^{Venus} mice. Two independent experiments, *N*=3 mice/group.

(I) TCF1$^{mCherry+}$IL-17A^{eGFP+} CD4 T cells were FACS-purified from SI LP of *Tcf7*^{mCherry}/*Il17a*^{GFP} mice (Ly5.1) and adoptively transferred into SFB-colonized WT mice (Ly5.2). TCF1 and IL-17 expression in transferred cells in SI LP was analyzed on Day 2 and Day 14 after transfer. Cumulative from several independent experiments, *N*=5 mice/group.

(J) TCF1$^{mCherry+}$IL-17^{GFP+}IL-10^{Venusneg} T_H17 cells were FACS-purified from SI LP of SFB-colonized or LI LP of *Citrobacter rodentium*-infected mice and stimulated *in vitro* as described in Methods. (Left) IL-10^{Venus} and IL-17^{GFP} expression in CD4 T cells. (Right) Proportion of IL-10^{Venus+} cells in TCF1^{mCherryneg}IL-17^{GFP+} T_H17 cells on Day 4. Three independent experiments, *N*=2–7 mice/group.

(K) PCA plot of bulk RNA-sequencing analysis of FACS-sorted TCF1$^{mCherry+}$IL-17^{GFP+} and TCF1^{mCherryneg}IL-17^{GFP+} T_H17 cells from SI LP of SFB-colonized or LI LP of *Citrobacter rodentium*-infected (*Crod*) mice. One experiment, *N*=2–4 mice/group.

(L) Number of differentially expressed genes (DEGs) in indicated pairwise comparisons of RNA-sequencing analysis in (K). One experiment, *N*=2–4 mice/group.

(M) Gene set-enrichment analysis of genes (Left) upregulated in TCF1$^+$ SFB T_H17 cells compared to genes upregulated in total SFB T_H17 cells or (Right) upregulated in TCF1$^+$ *Crod* T_H17 cells compared to total *Crod* T_H17 cells.

(N) Heatmap of DEGs arranged by the comparison between TCF1$^+$ SFB and TCF1$^+$ *Crod* T_H17 cells. SFB core signature anti-inflammatory genes in blue and inflammatory genes in red are listed on the right.

(O) Quantitative PCR for selected SFB signature genes in samples in K

(P) TCF1$^{mCherry+}$IL-17^{GFP+}IL-10^{Venusneg} T_H17 cells were FACS-purified from SI LP of SFB-colonized mice and stimulated *in vitro* in with or without 10 ng/ml IL-1β and 10 ng/ml IL23. (Left) IL-10^{Venus} and IL-17^{GFP} expression in CD4 T cells. (Right) Proportion of IL-10^{Venus+} cells in TCF1^{mCherryneg}IL-17^{GFP+} T_H17 cells on Day 4. Two independent experiments, each dot represents a technical replicate.

(Q) IFN-γ ELISA from *in vitro* cultures in (O). Two independent experiments, each dot represents a technical replicate.

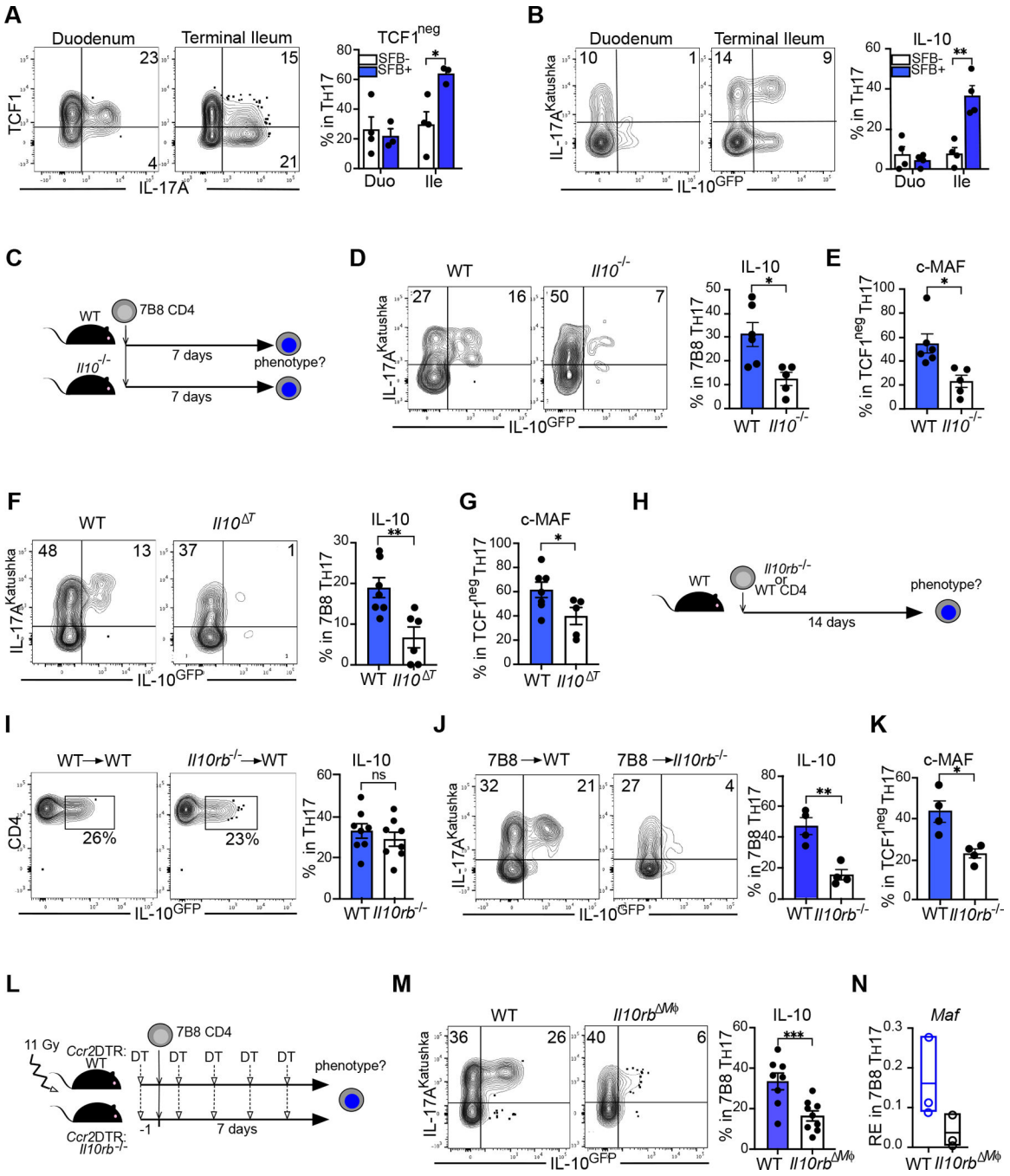

Figure 7. IL-10 signaling in intestinal Mϕs drives generation of anti-inflammatory commensal T_H17 cells in the terminal ileum

(A) Intracellular staining for TCF1 and IL-17 in duodenum (Duo) and terminal ileum (Ile) SI LP of SFB-colonized and SFB-negative WT mice. (Left) FACS plots from SFB-colonized mice, gated on $TCR\beta^+CD4^+$ lymphocytes. (Right) Proportion of $TCF1^{neg}$ effector cells in T_H17 cells, gated $TCR\beta^+CD4^+IL\text{-}17^+$ (Right). Two independent experiments, *N*=3 mice/group.

(B) Distribution of IL-10^{GFP+} T_H17 cells in duodenum (Duo) and terminal ileum (Ile) of SFB-colonized and SFB-negative *Il10^{eGFP}/Il17a^{Katushka}/Foxp3^{mRFP}* mice. (Left) FACS plots from SFB-colonized mice gated on TCRβ$^+$CD4$^+$lymphocytes. (Right) Proportion of IL-10^{GFP+} cells in T_H17 cells (TCRβ$^+$CD4$^+$IL-17$^{Katushka+}$). Two independent experiments, *N*=4 mice/group.

(C-E) Naïve SFB-specific 7B8 splenic CD4 T cells were purified from 7B8.Ly5.1 *Il10^{GFP}/Il17a^{Katushka}/Foxp3^{mRFP}* mice and adoptively transferred into SFB-colonized Ly5.2 WT or *Il10$^{-/-}$* mice (C). Expression of IL-10 (GFP) (D) and c-MAF (intracellular staining) (E) in SI LP one week after transfer. FACS plots in (D) gated on Ly5.1$^+$TCRβ$^+$CD4$^+$Foxp3^{mRFPneg} 7B8 CD4 T cells. Bar plots in (D) further gated on IL-17$^{Katushka+}$ 7B8 T_H17 cells. Bar plots in (E) further gated on IL-17$^+$ transferred 7B8 T_H17 cells. Cumulative of three independent experiments, *N*=5–6 mice/group.

(F, G) Naïve SFB-specific 7B8 splenic CD4 T cells were purified from 7B8.Ly5.1 *Il10^{GFP}/Il17a^{Katushka}/Foxp3^{mRFP}* mice and adoptively transferred into SFB-colonized WT or *Cd4^{Cre}/Il10$^{flox/flox}$* (*Il10$^{\Delta T}$*) mice. Expression of IL-10 (GFP) (F) and c-MAF (G) in SI LP one week after transfer. FACS plots in (F) gated on Ly5.1$^+$TCRβ$^+$CD4$^+$Foxp3$^{mRFP\text{-}neg}$ 7B8 CD4 T cells. Bar plots further gated on IL-17$^{Katushka+}$ (F) or IL-17$^+$ (G) transferred 7B8 T_H17 cells. Cumulative of two independent experiments, *N*=6–7 mice/group.

(H) Experimental schematic. Naïve splenic CD4 T cells were purified from *Il10^{GFP}/Il17a^{Katushka}/Foxp3^{mRFP}* (Ly5.2) WT or *Il10rb$^{-/-}$* mice and adoptively transferred into SFB-colonized Ly5.1 WT mice.

(I) IL-10 and c-MAF expression in transferred T_H17 cells in SI LP two weeks after transfer from the mice in (H). FACS plots and bar plots gated on Ly5.2$^+$TCRβ$^+$CD4$^+$Foxp3^{mRFPneg}IL-17$^{Katushka+}$ T_H17 cells. Cumulative of four independent experiments, *N*=8 mice/group.

(J, K) Naïve SFB-specific 7B8 splenic CD4 T cells were purified from 7B8.Ly5.1 *Il10^{GFP}/Il17a^{Katushka}/Foxp3^{mRFP}* mice and adoptively transferred into SFB-colonized Ly5.2 WT or *Il10rb$^{-/-}$* mice. IL-10 (GFP) (J) and c-MAF (K) expression in SI LP one week after transfer. FACS plots gated on Ly5.1$^+$TCRβ$^+$CD4$^+$Foxp3^{mRFPneg} transferred 7B8 T cells. Bar plots further gated on IL-17$^{Katushka+}$ (J) or IL-17$^+$ (K) transferred 7B8 T_H17 cells. Cumulative of two independent experiments, *N*=4 mice/group.

(L) Experimental schematic. Naïve SFB-specific 7B8 splenic CD4 T cells were purified from 7B8/Ly5.1 *Il10^{GFP}/Il17a^{Katushka}/Foxp3^{mRFP}* mice and adoptively transferred into DT-treated SFB-colonized Ly5.2 WT BM chimeras, reconstituted with 1:1 mix of BM from *Ccr2^{DTR}* mice and either WT or *Il10rb$^{-/-}$* mice. DT treatment was performed to deplete *Ccr2^{DTR}* macrophages as described in Methods.

(M) IL-10 (GFP) expression in SI LP one weeks after transfer from the mice in (L). FACS plots gated on Ly5.1$^+$TCRβ$^+$CD4$^+$Foxp3^{mRFPneg} transferred 7B8 CD4 T cells. Bar plots further gated on IL-17$^{Katushka+}$ transferred 7B8 T_H17 cells. Cumulative of two independent experiments, *N*=8–9 mice/group.

(N) Quantitative PCR of *Maf* transcripts in FACS-purified transferred SI LP 7B8 T_H17 cells (Ly5.1$^+$TCRβ$^+$CD4$^+$Foxp3^{mRFPneg}IL-17^{GFP+}) from the mice in (L). Cumulative of two independent experiments, *N*=3 mice/group.

KEY RESOURCES TABLE

REAGENT or RESOURCE	SOURCE	IDENTIFIER
Antibodies		
Rat anti-mouse CD4 antibody, RM4-5, BUV737	BD	#612844
TCR beta monoclonal antibody, H57-597, APC-eFluor780	eBioscience	#47-5961-82
Anti-mouse CD45.1, A20, PerCP-Cyanine5.5	Tonbo	#50-210-3580
Mouse anti-mouse CD45.2, 104, BV421	BD	#562895
Anti-Human/Mouse CD45R (B220), RA3-6B2, PerCP-Cyanine5.5	Tonbo	#65-0452-U100
CD103 Monoclonal antibody, 2E7, PE	eBioscience	#12-1031-82
CD11b Monoclonal antibody, M1/70, APC-Cyanine7	Invitrogen	#A15390
CD11c Monoclonal antibody, N418, PE-Cyanine7	eBioscience	#25-0114-82
Anti-mouse CD24 antibody, M1/69, BV510	BioLegend	#101831
CD62L Monoclonal antibody, MEL-14, FITC	eBioscience	#11-0621-82
Anti-mouse CD64, X54-5/7.1, APC	BioLegend	#139334
Anti-mouse CD69, H1.2F3, PE-Cyanine7	Tonbo	#60-0691-U025
CD127 monoclonal antibody, A7R34, PE	eBioscience	#12-1271-82
CD223 monoclonal antibody, eBioC9B7W, PerCP-eFluor710	eBioscience	#46-2231-82
Rat monoclonal anti mouse MHCII, M5/114.15.2, Alexa Fluor 710	Tonbo	#80-5321-U100
American Hamster monoclonal anti-gδTCR, GL-3,GL3 APC	eBioscience	#17-5711-82
CD366 monoclonal antibody, F38-2E2, APC	eBioscience	#17-3109-42
Mouse monoclonal anti FoxP3, FJK-16s, BV421	eBioscience	#404-5773-82
Fixable Viability Dye eFluor 506 (FVD)	Invitrogen	#65-0866-14
Rat monoclonal anti-mouse IFNγ, XMG1.2, APC	eBioscience	#17-7311-82
Rat monoclonal anti-mouse IL-17A, eBio17B7, FITC	eBioscience	#11-7177-81
Goat monoclonal anti IL-22 antibody (POLY5164)	Biolegend	#516406
Anti-mouse TIGIT, 1G9, BV421	BD	#565270
Anti-mouse CD152, UC10-4F10-11, PE-Cyanine7	Tonbo	#60-1522-U025
Anti-Human/Mouse CD44, IM7, APC	Tonbo	#50-210-2735
Rat monoclonal anti-mouse NKp46, 29A1.4, PerCP-Cyanine5.5	eBioscience	#46-3351-80
Rat monoclonal anti-mouse RORγt, PE	eBioscience	#12-6988-82
c-MAF monoclonal antibody, sym0F1, PE	eBioscience	#12-9855-42
Rat Anti-mouse GM-CSF, MP1-22E9, BV421	BD	#564747
TCF1/TCF7 Rabbit mAB, C63D9, APC	Cell Signaling Technology	#37636
Rat monoclonal anti-Vβ14 TCR, 14-2(RUO), Biotin	BD Bioscience	#553257
Rat Anti-mouse vb 14 T-Cell receptor, 14-2, FITC	BD	#553258
Rat monoclonal anti-mouse RORγt, PE	eBioscience	#12-6988-82
TotalSeq-B0301 anti-mouse Hashtag 1 Antibody	BioLegend	#155831
TotalSeq-B0302 anti-mouse Hashtag 2 Antibody	BioLegend	#155833
TotalSeq-B0302 anti-mouse Hashtag 3 Antibody	BioLegend	#155835
CD4 MicroBeads, mouse	Miltenyi Biotec	#130-117-043

REAGENT or RESOURCE	SOURCE	IDENTIFIER
Bacterial strains		
Segmented Filamentous Bacteria (SFB)	Kenya Honda	(Umesaki et al., 1995)
Citrobacter rodentium	ATCC	#51459
Bifidobacterium adolescentis	ATCC	#15703
Escherichia coli	ATCC	
Chemicals, cytokines, and recombinant proteins		
In VivoMAb anti-mouse IL-10R antibody (clone 1B1.3A)	BioXcell,	#BE0050
CD3e monoclonal antibody, functional grade (clone 2C11)	eBioscience	#16-0031-82
CD28 monoclonal antibody, functional grade (clone 37.51)	eBioscience	#16-0281-38
Mouse CTLA-4 Antibody (clone 63828)	R&D Systems	#MAB434-100
InVivoMAb anti-mouse LAG-3 (clone C9B7W)	BioXcell	#BE0174
InVivoMAB rat IgG1 isotyoe control (clone HRPN)	BioXcell	#BE0088
Recombinant Mouse IL-23 Protein	R&D Systems	#1887-ML
Recombinant Murine IL-1β	PeproTech	#211-11B
Corning Dispase, 100 mL	Corning (Fisher)	#354235
Roche Collagenase D 2.5g from C.histolyticum	Roche (Sigma)	#11088882001
Collagenase, type 1, powder	Gibco	#17018209
Deoxyribonuclease I from bovine pancreas, 1g	Sigma	DN-25
Hanks' Balanced Salt solution (HBSS), 10X	CORNING	#36320020
HyClone™ RPMI 1640 Medium, Sterile, pH 7.0 - 7.4, With L-glutamine, Liquid	Cytiva	SH30028.LS
Penicillin-Streptomycin (5.000U/ml)	Gibco	#15070063
β-mercaptoethanol	Sigma-Aldrich	#60-24-2
Natriumpyruvate (100 mM)	Gibco	#11360070
L-Glutamin (200 mM)	Gibco	#A2916801
MEM Non-Essential Amino Acids (100X)	Gibco	#11140068
Sodium Bicarbonate	SIGMA	#46H02825
Percoll®, Sterile, pH 8.5 - 9.5, Liquid	Cytiva	17-0891-09
Fetal Bovine Serum, Qualified, USDA approved	Thermo Scientific	#10437028
HEPES(1M)	Thermofisher	#15630-080
Phenol/Chloroform/Isoamyl alcohol (25:24:1), stabilized	Fisher Scientific	327115000
Ambion TRIzol reagent	Fisher Scientific	15-596-018
2-Propanol, ACS reagent, ≥99.5%	Sigma-Aldrich	#190764
Proteinase K	Lucigen	#MPRK092
Cell Trace Violet cell proliferation kit	Life Technologies	#34557
Ionomycin calcium salt from Streptomyces	Sigma-Aldrich	#10634
PMA, for use in molecular biology	Sigma-Aldrich	#P1585
Brefeldin A,from Penicillium brefeldianum, ≥99% (HPLC and TLC)	Sigma Aldrich	#B7651-5MG
Foxp3 / Transcription Factor Fix/Perm Concentrate (4X)	TONBO Biosciences	#TNB-1020-L050
Foxp3 / Transcription Factor Staining Buffer Kit	TONBO Biosciences	#TNB-0607-KIT

REAGENT or RESOURCE	SOURCE	IDENTIFIER
Flow Cytometry Perm Buffer (10X)	TONBO Biosciences	#TNB-1213-L150
Reinforced Clostridia Medium (RCM)	ThermoFisher	#CM0149
LB Broth	Gibco	#10855001
Critical commercial assays		
Qscript cDNA Super Mix, QuantaBio	VWR	#101414-108
2X Universal SYBR Green Fast qPCR Mix - 25 mL	ABclonal	#RK21203
IFN gamma Mouse ELISA Kit	Invitrogen	#BMS606-2
Lipocalin-2 (LCN2) Mouse ELISA Kit	Invitrogen	#EMLCN2
cOmplete, EDTA-free protease-inhibitor	Roche	#11836170001
Experimental models: Organisms/strains		
C57BL/6J, Room RB15	The Jackson Laboratory	#000664
Ptprc (CD45.1)	The Jackson Laboratory	#002014
Cd4^{CRE}	The Jackson Laboratory	#022071
7B8 TCR Tg	The Jackson Laboratory	#027230
Rag1$^{-/-}$	The Jackson Laboratory	#002216
Il17a^{GFP}	The Jackson Laboratory	#018472
Il10$^{-/-}$	The Jackson Laboratory	#002251
Il10rb$^{-/-}$	The Jackson Laboratory	#005027
Foxp3^{mRFP}	The Jackson Laboratory	#008374
Il10^{GFP}	The Jackson Laboratory	#008379
Rosa26^{YFP}	The Jackson Laboratory	#038215
Il17a^{Katushka}	R. Flavell, Yale U	N/A
Il10$^{flox/flox}$	A. Roers, TU Berlin	N/A
Il10^{Venus}	K. Takeda, Osaka U	N/A
Ccr2^{DTR}	E. Pamer, MSKCC	N/A
Tcf7-STOP mice	This Study	N/A
Oligonucleotides		
Il10 Fwd 5'-TTGGGTTGCCAAGCCTTATCG-3'	This Study	N/A
Il10 Rev 5'-AATCGATGACAGCGCCTCAG-3'	This Study	N/A
Maf Fwd 5'-GCGAAAGGGACGCCTACAAG-3'	This Study	N/A
Maf Rev 5'-AACAAGGTGGCTAGCTGGGA-3'	This Study	N/A
Il10rb Fwd 5'-TCAGTGCGACTTCTCTCATCTTTC-3'	This Study	N/A
Il10rb Rev 5'-AGGAGGTCCAATGATGGTGTCTT-3'	This Study	N/A
Areg Fwd 5'-TACTTTGGTGAACGGTGTGGAG-3'	This Study	N/A
Areg Rev 5'-GCGAGGATGATGGCAGAGAC-3'	This Study	N/A
Tox Fwd 5'-GTGTGAGGATGCCTCCAAGATCAA-3'	This Study	N/A
Tox Rev 5'-ACAAAGCATAGGCAGACACAGG-3'	This Study	N/A
Tcf7 Fwd 5'-GCGCGGGATAACTACGGAAA-3'	This study	N/A
Tcf7 Rev 5'-GCCTAGAGCACTGTCATCGG-3'	This study	N/A

REAGENT or RESOURCE	SOURCE	IDENTIFIER
Gzma Fwd 5'-GACACGGTTGTTCCTCACTCA-3'	This study	N/A
Gzma Rev 5'-CAATCAAAGCGCCAGCACAG-3'	This study	N/A
Ccl5 Fwd 5'-TGCTGCTTTGCCCTACCTCTC-3'	This Study	N/A
Ccl5 Rev5'-CCTTCGAGTGACAAACACGACT-3'	This Study	N/A
Ifng F 5-CACGGCACAGTCATTGAAAG-3'	(Kawano et al., 2022)	N/A
Ifng R-5-GCTGATGGCCTGATTGTCTT-3'	(Kawano et al., 2022)	N/A
Gapdh F 5-CCTCGTCCCGTAGACAAAATG-3'	(Atarashi et al., 2008)	N/A
Gapdh R-5-TCTCCACTTTGCCACTGCAA-3'	(Atarashi et al., 2008)	N/A
SFB F 5-GACGCTGAGGCATGAGAGCAT-3'	(Barman et al., 2008)	N/A
SFB R-5-GACGGCACGGATTGTTATTCA-3'	(Barman et al., 2008)	N/A
UNI F 5-ACTCCTACGGGAGGCAGCAGT-3'	(Barman et al., 2008)	N/A
UNI R-5-ATTACCGCGGCTGCTGGC-3'	(Barman et al., 2008)	N/A
Software and algorithms		
Flow jo_v10.6.2	BD	N/A
Bowtie2 v2.3.4	N/A	N/A
10X Genomics Cellranger toolkit v1.0.1	N/A	N/A
USEARCH v11.0.667	N/A	N/A
GraphPad Prism version 9.1	N/A	N/A
Other		
BD LSR Fortessa Flow Cytometer	BD	N/A
BD Aria, Floy Cytometer	BD	N/A
Zirconia/Silica Beads 0.1mm	Fisher Scientific	#11079101z
Miltenyi Biotec, Inc. LS Columns 25/PK	Miltenyil Biotec	#130-042-401
LightCycler® 480 System	Roche	N/A
Fisherbrand Razor Blades	Fisher Schientific	#12640
Insulin Syringes with Permanently Attached Needles	BD	#329420
Cell Strainer, Individual Package, 40 um, blue	VWR	#76327-098
Bead beater	Biospec	#1001
Beads cleanup	Beckman-Coulter	# A63881